Assessment of a Potential Radiological Attack

Investigation of Scenarios Pertaining to Contamination of Infant Milk Formula

Masayo Thorén

Master of Science Thesis
Chemistry
30 credits

Department of Chemistry
Faculty of Mathematics and Natural Sciences

UNIVERSITY OF OSLO

05 / 2017

Masayo Thorén

Assessment of a Potential Radiological Attack

Investigation of Scenarios Pertaining to Contamination of Infant Milk Formula

Master of Science Thesis
Chemistry
30 credits
05 / 2017

Department of Chemistry
Faculty of Mathematics and Natural Sciences
University of Oslo

2017

Assessment of a Potential Radiological Attack
Investigation of Scenarios Pertaining to Contamination of Infant Milk Formula

Masayo Thorén

http://www.duo.uio.no/

Printing: Reprosentralen, University of Oslo

Abstract

The purpose of this work is to systematically assess the consequences of a potential radiological attack on processed food in a production facility. Infant milk formula (IMF) is specifically chosen as the case of investigation. Three different radionuclides, ^{90}Sr, ^{137}Cs and ^{241}Am, are chosen as sources of contamination for the assessment.

The assessment of the consequences of an attack is limited to negative health effects, i.e. mortality or morbidity. It is found that a considerably large number of infants would potentially receive negative health effects due to ingestion of radionuclides in the contaminated IMF (depending on the activity used at the time of contamination, as well as the contamination scenario). However, in the case of contamination at mortality and morbidity level, the radioactivity from contaminated IMF is calculated to be detectable during its production phase. This is achieved using a NaI(Tl) detector on the outside of an IMF packaging (a can) during the production. In the case of contamination at permissible level, the detector would only alarm the abnormality for the ^{137}Cs source. This investigation has also found that radioactive sources that are easily accessible to the general public are possible to use in such scenarios with some effect. This finding further encourages the related industries to practice preparedness against the possibility of contamination events using radioactive materials.

Acknowledgement

When I knocked on Professor Jon Petter Omtvedt's door at the Nuclear Chemistry section at University of Oslo, I was in many ways knocking on the door to my future. I told him with a lot of hesitation that I wanted to contribute to world peace; a subject that may not be directly associated with chemistry, nor nuclear chemistry in academics. He looked me in the eye and asked me directly: you don't think that nuclear chemistry can contribute to peace? At that moment I knew that I had come to the right place. Without Professor Omtvedt, I would never have pursued my personal commitment through this work and through my study at the University of Oslo. My deepest appreciation, from the bottom of my heart, goes to Professor Omtvedt.

I would also like to thank Dag Øystein Eriksen for his advice and encouragement, and Hans Vigeland Lerum for his support and assistance throughout the course of my study. Furthermore, I would like to acknowledge the administration at the Department of Chemistry, who gave me full understanding and empathy regarding personal events that took place during my study (work, sickness and maternity leave), and arranged my study progression fairly. I would also like to acknowledge the administration at the Department of Physics, who allowed me to attend two of their courses. These courses have played an important role in writing this work.

Lastly, I would like thank my family for their deepest understanding and unlimited amount of support. My husband, Anders, has encouraged me ever since I applied for the Master's program at the university, throughout my study, and during this work. His contribution has been essential to complete the Master's program. Our son, Leon, has been a great inspiration and motivation during my study and this work (he even attended some classes with me). He was the reason I never gave up throughout the many difficulties I encountered. Our daughter, who has not yet come to this world, has been following this work from inside my belly. She has also been a great motivation, equally to that of Leon.

As a mother, I want to ensure everyday peace to my son, daughter and family. That is a human right that they and all of us deserve equally. I strongly hope that this work, as well as my future works on this subject, will make a difference and ultimately contribute to world peace.

Table of Contents

1 Introduction

The Fukushima Daiichi nuclear accident in March 2011 was one of the worst and most devastating experiences in my life. As it unfolded on TV and Internet in front of me in Norway, thousands of miles away from home, I kept feeling helpless and saddened. Public fear for health effects from the released radiation then began flourishing. A fear that quickly led to discrimination of the people from Fukushima. The very people who had already suffered the Tsunami and the nuclear accident. Public fear led to panic. I felt ill seeing my nation suffering in such way. The Fukushima accident, in addition to the nuclear bombs dropped on Hiroshima and Nagasaki in 1945, resulted in one of the world's worst nuclear disasters to date. This experience became the driving force behind my study, and in turn this work. Protecting the public from nuclear and radiological threats has become my commitment.

In this work, a virtual case of deliberate radiological contamination is investigated. Processed food during production was chosen as the route of contamination. The production process makes it possible to evenly contaminate food items that are easily accessible to the public. If the contamination is a terrorist act, the impact can be greatly enhanced by choosing a target that has symbolic value to the general public or that can strike primal emotions in the public [1], besides the direct negative health effects. In the latter case, Infant Milk Formula (IMF) could be such a target. IMF is a processed food that is designed to feed infants. The form of IMF is often powder or liquid. It is prepared for feeding either by mixing with water (in the case of powder) or by diluting with water (in the case of liquid). In this work, I have chosen the production line of a powdered IMF factory as the target of contamination.

In the case of an emergency, *preparedness* and *response* would be of equal importance. The focus of this work is on preparedness. In preparedness, *risk assessment* and *prevention measures* are necessary to minimize the consequences of the emergency if/when it takes place. In terms of risk assessment related to the chosen scenario, the degree of negative health effects to infants, i.e. conditions that lead to early death and conditions that are non-lethal, and the potential number of infants affected are estimated. When it comes to preventive measures, it would be ideal if the contamination event can be prevented ahead of time. However, in the case of an event already occuring, contaminated IMF must be prevented from being ingested by infants. The best approach would be to detect the contamination during the production phase, before distribution occurs. Several different methods for how to detect contamination in a manufacturing facility are investigated in this work, and their respective level of effectiveness are discussed and assessed. To motivate and encourage the preparedness for this type of deliberate contamination, a discussion over potential and probability of contamination is also included.

It is my highest hope that this work will shed light on how to counteract radiological threats against the food industry, and that it will bring awareness and implementation of precaution measures to all other related industries.

2 Background

Warfare seems to be as old as human history itself, but modern technology has brought the resulting destruction and suffering to disheartening heights. In former times, madmen would attack others furiously with rather simple weapons. However, in today's world, the use of modern technology can cause catastrophic results: Methods of mass destruction and mass-murder are available to individuals or small groups, if they set their mind on it.

Looking back on history, the uses of chemical and biological weapons have been reported as early as in ancient Greece, the fifth century B.C. [2, 3]. Nuclear weapons, on the other hand, had their destructive premiere in more recent history; in the 1945 bombings in Japan, during the World War II. Radiological weapons, as further described later, have not yet been used. The poisoning of Alexander Litvinenko (a former Russian spy) using ^{210}Po in 2006 seems to have been recognized as an assassination rather than a radiological attack.

The collective term, CBRN, is an acronym that stands for Chemical, Biological, Radiological and Nuclear [4]. CBRN attacks have widely been recognized in academics for decades. Among them, the Tokyo subway sarin attacks in 1995 and the Anthrax attacks (in Washington, D.C., West Palm Beach and New York City in USA) in 2001 are the ones that have been most commonly written about. These incidents were alarming and showed the reality of the threats from CBRN attacks to the Western world. The threat of attacks with unconventional means became even more recognized after the September 11th attacks in the US in 2001. This was an event that dramatically displayed the existence of groups with the desire to cause the greatest of harm and damage to the world. Unfortunately they also demonstrated that they possess sufficient financial backing and human resources to actually carry out an attack [5, 6]. CBRN attacks may be characterized by three types of large-scale impacts [7]:

1) Physical impact resulting in injuries and deaths;
2) Social impact resulting in the change of public confidence and the disruption of daily life; and
3) Economic impact resulting from the direct damage as well as the indirect damage that is caused by the physical and social impacts.

In this work, the physical impact will be the primary focus.

Perpetrators[1] make their choice of a certain method of attack, i.e. CBRN attacks or traditional attacks (using conventional weapons). CBRN attacks may be attractive to some perpetrators due to the potential of causing mass casualties, significant long-term economic loss [8], considerable political damage, traumatic psychological impact that is not possible to achieve by traditional attacks [9], and/or the ambition to obtain media attention similar to the September 11th attacks [8]. A study done by Ivanova and Sandler, that investigated the relationship between regime characteristics and the likelihood of CBRN incidents, concludes that the likelihood of CBRN attacks being carried out to a

[1] CBRN attacks are often connected to terrorism, even though the definition of *terrorism* among academics and other professionals vary. In this work, the groups of people and individuals who plot CBRN attacks are all referred to as *perpetrators*.

country increases with degree of implemented democratic processes in society and wealth [6, 8]: the Western world may therefore be at a high risk of receiving such an attack.

As mentioned earlier, radiological attacks are the only type of CBRN attacks which has not yet been successfully conducted. In order to carry out radiological attacks, the most commonly known method is the use of Radiological Dispersion Devices (RDD); also known as dirty bombs. This method has never been successfully accomplished; even though some attempts have been reported, such as by the Chechen rebels in 1997 [10]. RDD is a conventional explosive which is combined with radioactive material. The conventional explosive can be such as the one used in the bomb attack by Anders Breivik in July 2011 in Oslo, Norway. In general, radiological attacks do not require state of the art technology. Any kind of radioactive material, e.g. from educational/research institutions, commercial industries or medical facilities, can be used to accomplish such a attack. Radiation protection is necessary to prevent radiological health effects to a person handling radioactive material; yet, such concern may not be much relevant to the perpetrators, who could have strong will to sacrifice their own lives to carry out the attack.

Andersson et al. relates a consequence of RDD to a radiological accident that occurred in Goiânia, Brazil in 1987 [11]. A source containing ^{137}CsCl, equivalent to 51 TBq, was found at a scrap yard [12]. The source had a mysterious glow in blue to it and fascinated residents in the village [13]. This resulted in a large contamination area, which is calculated as equivalent to that of a successful dirty bomb [11, 14]. Four fatalities were reported within weeks [12]. However, regardless to the number of fatalities, the accident resulted in massive social disruption and enormous economic loss. Similar incidents, and thus similar consequences, may happen elsewhere. Yet, it may not be accidental: it may be deliberate such as through a radiological attack. For this reason, it is necessary for emergency and safety organizations, around the world, to be prepared and have personnel trained to handle such incidents. The first step is to evaluate the threat and the consequences of such an attack. This work will hopefully contribute to such an evaluation.

In 2001, three residents of Tsalenjikha in Georgia found two radioactive sources in a forest. Each source contained ^{90}Sr with activity of about 780 TBq at the time of discovery (initial activity of each source was assumed to be 1295 TBq in early 1980s when produced) [15]. It was concluded that these ^{90}Sr sources originated from Radioisotope Thermoelectric Generators (RTG) [15]. These were widely distributed along the northern coast line of the former Soviet Union to act as power sources for remote applications (like lighthouses) during the period [16]. If such a source gets into the hands of perpetrators, it may be used against the general public. In 1997, the Norwegian government started to replace the ^{90}Sr sources equipped with RTGs in Russian lighthouses. They were replaced with non-radioactive power sources [17], and the project has now been completed.

Threats of radiological attacks have been growing substantially over time. An example would be British resident, Dhiren Barot, who was arrested in 2004 for plotting the construction of a RDD using ten thousand commonly used household smoke detectors, that are equipped with ^{241}Am source [18]. The RDD was reportedly planned to be detonated in a subway. Barot was a top member of a British terrorist organization with ties to the terrorist organization Al Qaeda [19]. The possible intent for radiological attacks has also recently been shown by another terrorist organization ISIS. In the end of 2015, surveillance video footage of a high-ranking employee at a Belgian nuclear facility was found during law enforcement investigations following the Parris attack in November 13 (which involved several mass shootings and suicide bombs at multiple locations and resulted in 130 fatalities) [20]. This official had full access to secure areas of a nuclear research facility. Experts have speculated that

this incident was part of a plot to abduct or blackmail the official in order to obtain radioactive material from the facility. According to the International Atomic Energy Agency (IAEA), their Incident and Trafficking Database (ITDB) contained 2889 confirmed incidents related to radioactive material between 1993 and 2015 [21]. These incidents include a wide range of activities, from neglect to criminal activity for personal gain, such as illicit trafficking, thefts, losses, unauthorized possession and recoveries of the radioactive material. The degree of these incidents associated directly to plots of radiological attacks is unknown. In April 2016, EU and NATO officially stated a "justified concern" that ISIS was plotting radiological attacks, as well as other CBRN attacks, here in Europe [22].

There are a variety of methods, other than RDD, that can be used in radiological attacks. Therefore, different consequences are expected for each type of radiological attack. The consequences may differ largely with route of exposure and the ability to detect the first signs of an attack. In an RDD attack, the major route of exposure is external from the environment and internal from inhalation of dust. In the case of inhalation, the radionuclides inhaled are either removed from the lung immediately due to exhalation or retained in the lung. A fraction of retained radionuclides are then transferred to the throat and ingested [23]. The original attack is "demonstrative", i.e. highly likely to be noticed due to an initial explosion. If appropriate emergency response is carried out, i.e., using necessary radiation protection procedures, it is estimated that the attack is not likely to cause immediate health effects due to radiation [14]. In the majority of literature, radiological attacks are, even when successfully carried out, expected to cause a very small number of casualties compared to that of chemical, biological and especially nuclear attacks. However, the cases/scenarios described in these literature mainly focus on methods such as RDD. Deliberate contamination of foods/drinks, for example, where the major route of exposure is internal through ingestion, have not been widely discussed. In such case, the original attack may be "stealth-like", i.e. it may not be noticed for quite some time. As the consumption of foods/drinks per person increases; so does the radiation dose. In addition, the distribution of the contaminated foods/drinks can increase the potential of number of people affected. Thus, if this type of radiological attack is successful, it has great potential to cause health effects on a scale comparable to that from chemical and biological attacks. Deliberate contamination of water supplies and reservoirs has been discussed, and most of the literature have concluded that the method would likely be unsuccessful due to a large dilution factor and water purification features that normally are in place to ensure clean and good quality of water [9]. Tofani and Bartolozzi have investigated a case of deliberate radiological contamination against a water reservoir. In their work, committed collective dose, the sum of lifetime absorbed doses to a population from ingestion of radionuclides, is approximately estimated as 80 man Sv for the population of 150 000 people. Therefore, the expected number of fatality in the population per lifetime due to stochastic effect, e.g. cancer, is estimated as 5. However, the water purification features is excluded [24].

3 Objectives

Two primary questions must be answered:

1) What kind of negative health effects, i.e. lethal and non-lethal conditions, would result from a contamination event using radioactive sources of different radionuclides and activity levels?
2) How radioactive material from any kind of contamination event can reach its target group?

A contamination event can be carried out using any type of radioactive sources at any activity levels. However, no actual radiological attacks have been carried out. In this work, there is no experimental work conducted. Therefore, the case of a virtual event is only considered in this work. How easy or difficult it would be to carry out the attack, such as to obtain specific radioactive sources of specific quantities and the health hazards to perpetrators while preparing and performing the event due to radiation, are not considered in these primary questions. In the case that powdered IMF is contaminated without any notice, the primary focus should be to prevent the contaminated IMF from being distributed. This requires rapid on-line detection procedures to be performed routinely at site, i.e. the manufacturing facility.

An additional question then arises:

3) What is the minimum activity necessary to be detectable in a final product, when a radioactive source is physically added to the production, i.e. at the time of contamination?

Perpetrators may claim a radiological attack in order to simply obtain media attention. However, the radioactivity used for contamination, if any, must be sufficiently large in order for the attack to be confirmed, even if the amount of radioactivity is far from enough to cause any type of negative health effects.

Lastly, two final questions arise:

4) Are the contamination events discussed in this work realistic and possible to carry out?
5) If so, in what degrees compared to other type of attacks, from chemical, biological and nuclear attacks to traditional attacks?

The investigation pertaining to this includes chemical dissolution of initial radioactive sources.

To answer the primary questions, three radioactive sources, in different amounts, are selected based on availability of the source; availability in large quantities; and past trafficking and other incidents [25]. A virtual IMF manufacturing facility was constructed for this work, based on general information about food factories and typical equipment that are for sale. Four different contamination scenarios are set for the facility. Based on these setups, as further explained in **Section 5**, health effects resulting from the radioactive sources at selected levels of activities are assessed for each contamination scenario. This demonstrates the potential health consequences of a radiological attack on processed foods. Minimum activity of each source necessary to cause health effects to an infant is then calculated for mortality and morbidity. Investigation moves on to detection of contamination using the three different activity levels: selected level (as mentioned above); mortality

level; and morbidity level. Three different “detection methods” are investigated: a solid scintillation detector placed at a packaging site; health effects to workers at certain points in the manufacturing facility; and heat generation due to radioactive decay energy at specific points of manufacturing. Count rates measured using a solid scintillation detector are calculated in order to assess if placement of conventional detector(s) at site can alarm about a radioactive contamination before final products are distributed. Absorbed dose rate externally received by workers is calculated in order to assess if any deterministic health effects would cause particular symptoms that can alarm about abnormalities inside the facility. Heat-generation rate is calculated in order to assess if any temperature increase can be detected to generate warnings about abnormality during manufacturing.

For question 3, common laboratory detectors such as a High Purity Germanium (HPGe) detector or a Liquid Scintillation Counter (LCS) are selected to investigate minimum detectable activity (MDA) of radionuclides in powdered IMF. Minimum activity necessary at the time of contamination is then calculated based on the MDA of each radionuclide.

For the two final questions, methods for chemical dissolution of selected radioactive sources are investigated. This is mainly based on by the Tokyo Sarin attacks in which the sarin gas used was chemically synthesized by the perpetrators themselves in their own facility. Lastly, the potential of the radiological attack investigated in this work is discussed, with comparison to other CBRN attacks and traditional attacks as well as the September 11^{th} attacks that resulted in 2977 fatalities in total where 2753 of those occurred in the World Trade Centers [26].

In this work, investigations are scientifically conducted and conclusions are made based on numerical facts and results. Therefore, the behavior of different perpetrators; the preference of a particular impact such as health, economic or social impact by the perpetrators; the vulnerability of manufacturing points to deliberate contamination; and precise estimation of expected consequences to the general public are out of scope of this work.

4 Theory

Radiation that has the ability to ionize matter is called *ionizing radiation*. Among them, α particles, β particles, γ rays and bremsstrahlung (electromagnetic radiation emitted when β particles interact with matter) are of specific interest in this work. It is written based on an assumption that readers have a basic knowledge of radioactivity.

4.1 Interaction of β Particles with Matter

When β particles interact with matter, the particles lose their energies in two different ways: 1) through Coulomb interactions, i.e. the excitation and ionization of atoms or molecules that constitute the matter; and 2) through a radiative deceleration when electrons are deflected by the positively charged atomic nuclei of specified matter, i.e. generation of *bremsstrahlung*. The energy lost due to the radiative interaction can be estimated using *radiation yield* for bremsstrahlung. The energy lost due to both of Coulomb and radiative deceleration can be estimated using *stopping power*.

4.1.1 Bremsstrahlung

When charged particles such as β particles (electrons ejected from disintegrating nuclei) interact with matter, they may in principle be deflected by any other charged particle through the repulsive and attractive forces that occur between charged particles, the Coulomb interaction. Most of these interactions occur between electrons in the block of matter and the incoming electron. Due to their equal mass, this will not deflect the path of the incoming electron very much. However, it will be gradually slowed down by the transfer of small amounts of energy to each electron it passes. However, if the incoming electron passes close to an atomic nucleus, the charge is high and the nucleus has much higher mass. In this case, the electron will be significantly deflected from its original path, and something which requires a certain amount of electromagnetic radiation, by the laws of physics, will be ejected. Such electromagnetic emission is commonly called bremsstrahlung, using the German expression for the "breaking" effect.

Any charged particles that are deflected generate bremsstrahlung. Bremsstrahlung is not emitted isotropically, as it has a strong angular dependency to the path of the β particle. As the energy of the β particle increases, bremsstrahlung tends to be emitted closer to the path of the β particle. For example, the angle of bremsstrahlung generated from β particles with the energy of 50 keV stays within the range between +60° and -60° from the direction of the β particles. The angular range is reduced to ±30° when bremsstrahlung is generated from β particles with 500 keV of energy [27].

4.1.2 Radiation Yield for bremsstrahlung

The fraction of the β particle energy lost due to generation of bremsstrahlung is called bremsstrahlung radiation yield, Y_i. Bremsstrahlung is important for the topic of this work, since it is more penetrating than β particles. Therefore, in many cases, bremsstrahlung is the most practical

way to search for a concealed source that emits β particles but not γ rays, even though the intensity of the bremsstrahlung is considerably less than the β particles itself. In this work, bremsstrahlung radiation-yield is hereafter simply referred to as *radiation yield*, although this term might have other meanings in other settings.

The radiation yield used in the calculation of absorbed doses (as explained later) in this work is shown in **Table 21** in **Appendix C**. The amount of energy converted from the β particles into bremsstrahlung photons can be calculated using the values shown in **Table 21**.

4.1.3 Stopping Power

The energy of a β particle lost along its path in matter, due to the Coulomb interactions, is specific to the energy of the β particle. The stopping power is defined as:

$$S = \frac{dE}{dx}$$

Where dE is energy loss of the β particle traversing a path of length dx. The value of S is specific to the material composition of the absorber. S is also dependent on the electron density of the material. By introducing the density of the material ρ, the value of S is often specified as *mass stopping power* $\frac{S}{\rho}$, which is a constant. The mass stopping power, as well as the density of each material used in the calculation, is shown in **Table 22** in **Appendix C**. The penetration length of a β particle in specified matter can be calculated using the energy of the β particle and the values shown in **Table 22**.

4.2 Interaction of γ Rays with Matter

When a γ ray collide with an electron which is bound to atoms in matter, the energy of the γ ray minus the binding energy of the electron (which is negligible compared to the γ ray energy) will be conserved by transferring it to the electron. The intensity of the γ rays after the interacting with the matter can be estimated using *absorption coefficient*.

4.2.1 Absorption Coefficient

The intensity of γ rays that penetrate matter, I, exponentially decreases with the penetrating length of the γ rays in the matter. The following relationship exists:

$$I = I_0 \cdot e^{-\mu x}$$

Where μ is an absorption coefficient, I_0 is the initial intensity of the γ rays and x is the penetrating length of the γ ray in matter. μ, in the same way as S, is a material specific value. μ is also dependent on the electron density of the material. Therefore, in the same way as S, the value of μ is often specified as a *mass absorption coefficient* $\frac{\mu}{\rho}$, which is a constant. The mass absorption coefficients used in the calculation is shown in **Table 23** in **Appendix C**. The intensity of γ rays after penetrating specified matter of a given thickness can be calculated using the values shown in **Table 23**.

4.3 Absorbed Dose

Absorbed dose is the energy deposited in a given amount of matter, such as body tissue. The unit for an absorbed dose is Gray (Gy), and is equivalent to J/kg. Charged particles deposit their energies in a short distance, or *densely*, while electromagnetic waves impart their energies *thinly*. If the radiation energy is deposited densely within a smaller volume of body tissue, the damage to the tissue caused by the radiation can be enhanced compared to the energy deposited thinly within a larger volume. This is because the local concentration of deposited energy overwhelms the repairing mechanism of the cells in the small volume of tissue. Therefore, densely deposited radiation causes more damage than when it is thinly deposited. However, this is not taken into account by the absorbed dose. Thus, the absorbed dose distribution within the body tissue ranges from practically homogeneous to highly heterogeneous, depending on the type of radiation. To overcome this issue and to capture the relative effectiveness of different types of radiation in inducing biological damage, relative biological effectiveness (RBE) is applied. RBE is an experimentally or clinically derived value that is given as a ratio between two different absorbed doses that induce the same deterministic biological effect to a cell. One of the absorbed doses is given from reference radiation, and the other is given from the radiation in question. The International Commission of Radiological Protection (ICRP) defines the use of REB to reflect only to the deterministic effects, such as the effects investigated in this work [28].

The absorbed dose is a measured value. However, it can be estimated using *coefficients*. Coefficients provide a relationship between amount of a specific radioactive material (in Bq) and the resulting absorbed dose per unit time. In this work, two different coefficients are used: one for the absorbed dose rate given from internal exposure, i.e. ingestion of radionuclides; and the other for the absorbed dose rate given from external exposure to γ rays. The coefficients for internal and external exposures used in this work are referred to as *absorbed dose rate coefficient for ingestion* and *absorbed dose rate coefficient for external exposure*, respectively.

4.3.1 Absorbed Dose Rate Coefficient for Ingestion

Absorbed dose rate coefficient for ingestion (in Gy/day·Bq) is used in this work [29]. The coefficient is given to each day from initial ingestion of radionuclides, starting on Day 1, as shown in **Table 24** in **Appendix C**. The sum of the absorbed dose rate coefficients from Day 1 to Day N equals the total absorbed dose received from unit activity by the end of Day N since Day 1, i.e. the day of ingestion of the radionuclides. Therefore, in order to calculate the absorbed dose received from, for example, ingestion of radionuclides of unit activity for 3 consecutive days, the sum of the coefficients of Day 1, 2, and 3 (which represents the absorbed dose by the end of Day 3 from the ingestion on Day 1), that of Day 2 and 3 (which represents the absorbed dose by the end of Day 3 from the ingestion on Day 2) and the coefficient of Day 3 (which represents the absorbed dose by the end of Day 3 from the ingestion on Day 3) must be added. The value of the coefficient is age and organ specific. The coefficient for infants (less than the age of 1 year) is used in the calculation. The coefficient takes into account the dose contribution from all of the daughter nuclides (of a specified radionuclide) occurring after ingestion. However, at the time of ingestion, the specified radionuclide is assumed to be the only existing radionuclide [30].

4.3.2 Absorbed Dose Rate Coefficient for External Exposure

Absorbed dose rate coefficient for external exposure consists of two different sub coefficients: 1) exposure rate constant Γ and 2) conversion factor between exposure rate in air and dose rate to tissue f [31]. Γ in C·m^2/kg·Bq·h gives the exposure rate in air X in C/kg·s at the point, where the absorbed dose rate D to the person in question, as:

$$X = \Gamma \times \frac{A}{d^2}$$

Where A is an activity of the external γ source in Bq and d is the distance between the source and the person in m. f in Gy·kg/C then converts X into D received by the person as:

$$D = X \times f$$

Thus, D is given in Gy/h. Γ and f used in the calculation is shown in **Table 25** in **Appendix C**. They are given based on the size of an adult weighing 70 kg, from a point source: the γ source with a specific activity is assumed to be placed at a single point. The γ rays emitted from a specified radionuclide with energy above 15 keV are taken into account. The dose contribution from all of the daughter nuclides (of a specified radionuclide) is not taken into account, except ^{137}Cs whose daughter ^{137m}Ba has sufficiently short half-life. Occurrence of Bremsstrahlung is neglected [31].

4.4 Assessment of Health Effects of Radiation

When radiation ionizes a biological matter — a body —, the ionization may result in double-strand breaks (DSBs) of DNA in a cell. The biological process in the cell attempts to repair the DSBs. However, some DSBs are either non-repairable or only repairable into lethal chromosomal aberrations. These result in death of cells or mutation of damaged cells. The body replaces these dead cells as a part of a natural process. However, the replacement of the dead cells may not occur in reasonable time, if a large number of cells are lethally damaged in a short time. Considerable amounts of such cell death, if concentrated, can induce tissue reactions; this is known as *deterministic effects*. Some DSBs are repairable into chromosomal aberrations [32] that may result in gene/chromosomal mutations. Such mutations significantly contribute to an increase in cancer risk; this is known as the *stochastic effect*. Deterministic effects are characterized by threshold: the absorbed dose capable of sustaining tissue reactions into a clinical expression [28]. The severity of the effects, above the threshold, increases with higher doses. In the case of the stochastic effect, the probability of occurrence of this effect for higher doses has a linear relation to dose, i.e. greater in a higher dose. However, the severity of the effect is independent of dose. In this work, health effects are assessed only by deterministic effects. This is based on an assumption that perpetrators carry out a radiological attack where they want effects to become apparent quickly (within days to weeks).

4.4.1 Type of Deterministic Effects

Among the different types and levels of deterministic effects, the ones that are relevant in this work are prodromal syndrome, hematopoietic syndrome and gastrointestinal syndrome. The prodromal syndrome is the term used to describe specific symptoms that may indicate the onset of disease. Prodromal syndrome can be caused due to absorption of radiation, both internally (in the abdomen) and externally (in the head and torso areas). Prodromal syndrome results in morbidity, i.e. the condition of worsened health yet not being lethal. Morbidity may reduce quality of life, such as seen

in disability. Symptoms of the syndrome include vomiting and diarrhea from the ingestion of radionuclides and anorexia, nausea, fatigue, vomiting and diarrhea from external exposure [33]. Hematopoietic syndrome, also known as bone marrow syndrome, is caused by death of blood cells due to the absorption of radiation in the bone marrow. The hematopoietic syndrome results in mortality, i.e. the death. Symptoms of this syndrome include bleeding and inability to fight infection [33]. Gastrointestinal syndrome is caused due to the absorption of radiation in the colon, if radionuclides are ingested. The gastrointestinal syndrome also results in mortality. Symptoms of the syndrome include vomiting, diarrhea and gastrointestinal bleeding [33]. The threshold of all of the syndromes is shown in **Table 1**. In the calculation, the absorbed dose to the large intestine is used for the gastrointestinal syndrome. The sum of absorbed dose in the stomach, the small intestine and the large intestine is used for the prodromal syndrome caused by ingestion of radionuclides. The absorbed dose to the bone marrow is used for the hematopoietic syndrome. The absorbed dose rate coefficient is calculated for each syndrome and is shown in **Table 24** in **Appendix C**. The RBE value of 2 is applied for the absorbed dose given to the bone marrow from ^{241}Am contributed by α particles [33].

Table 1: Threshold of the different deterministic effects is shown. The thresholds for the syndromes that result in mortality (shown above with *) are based on the effects that occur in 1% of adults, while that for morbidity is based on 1% [33]. Since the threshold is derived based on the tissue reactions in adults, the values are not specific to infants.

Deterministic effect	Region/organ	Threshold (Gy)
Prodromal syndrome (ingestion)		
Vomiting	Abdomen	0.49
Diarrhea		0.55
Hematopoietic syndrome	Bone marrow	1.5*
Gastrointestinal syndrome	Colon	23*
Prodromal syndrome (external exposure)		
Anorexia	Head and torso	1.0
Nausea		1.4
Fatigue		1.5
Vomiting		1.8
Diarrhea		2.3

4.5 Temperature Increase in Matter Caused by Radionuclides

In this work, temperature increase of IMF that is contaminated with radioactive sources during its production process is investigated. This is to assess if the temperature increase can be used to detect radioactive sources.

Radionuclides can generate significant amount of heat by absorbing the energy carried by emitted particles from the disintegration process. S*pecific power* is the power produced due to disintegration per unit mass of a radioactive compound. *Specific heat* is the energy necessary in order to raise the temperature per unit mass of the matter by 1 °C. The rate of the temperature increase of the matter

caused by the radioactive compound in the matter is therefore calculated using specific power and the specific heat.

4.5.1 Specific Power

Specific power used in this work is given with the unit of W/g. The unit for power, W, is equivalent to J/s. Specific power is often given for a specific radioactive compound. However, it can be converted into that for a radionuclide which forms the compound, by using the mass ratio of the radionuclide to the compound. This is if the specified radionuclide is the only radionuclide that exists in the compound. Thus, the specific power of the radionuclide is given in J/s·g, regardless of type of compound. Specific activity A_{Spec} of the radionuclide in Bq/g is given as:

$$A_{Spec} = \frac{ln2 \cdot NA}{t½ \cdot M}$$

Where N_A is the Avogadro constant, $t_{1/2}$ is the half-life of the radionuclide in s and M is the atomic mass of the radionuclide. The energy generated per unit time and unit activity of the radionuclide, in J/s·Bq, is then given by division of the specific power by the specific activity of the radionuclide. The specific power used in this work is shown in **Table 2**.

Table 2: Specific power in W/g used in this work is shown. For ^{241}Am, the value is given for the radionuclide, not in a form of compound.

Compound/nuclide	Specific power (W/g)
^{137}CsCl	0.122 [34]
$^{90}SrTiO_3$	0.256 [35]
^{241}Am	0.11 [36]

4.5.2 Specific Heat

Specific heat used in this work is given with the unit of cal/g·°C. 1 cal is 4186 J. Therefore, the value of specific heat can be converted into the unit of J/g·°C using the conversion rate. The specific heat used in this work is shown in **Table 3**.

Table 3: Specific heat in cal/g·°C used in this work is shown for each compound. IMF represents the solid compounds in the IMF mixture during its manufacturing process.

Compound/nuclide	Specific heat (cal/g·°C)
Water	1.00
IMF	0.363 [37]

4.6 Minimum Detectable Activity

In this work, Minimum Detectable Activity (MDA) of ^{90}Sr, ^{137}Cs and ^{241}Am are taken from references and used in the calculation. The MDA is influenced by many parameters such as the type of detector used, counting time and the geometry between the sample and the sensitive part of the detector.

Optimizing each parameter is important. However, in the case of an radiological attack (such as the hypothesis in this work), fast detection of radionuclides is the main priority. ^{137}Cs and ^{241}Am emit γ rays, while ^{90}Sr emits no γ rays but β particles instead. The activity of each radionuclide is assumed to be detected using common laboratory detectors. Therefore, a High Purity Germanium (HPGe) detector is chosen for the detection of ^{137}Cs and ^{241}Am, and a Liquid Scintillation Counter (LSC) is chosen for the detection of ^{90}Sr.

4.6.1 MDA Obtained by HPGe Detector

The values of the MDA for ^{137}Cs and ^{241}Am used in this work, as shown in **Table 4**, are taken from a reference [38] The MDA given in the reference is determined based on the capability to identify an unknown radionuclide [39]. The MDA obtained with the counting time of 5 hours using a P type HPGe detector, which is the most commonly used HPGe in laboratories for counting, with the relative efficiency of 80% is used in the calculation. In the reference, the radionuclides are separately dissolved in water.

Table 4: MDA of ^{137}Cs and ^{241}Am in a sample using a HPGe detector with a counting time of 5 hours. The MDA is obtained from a P type of HPGe detector with the relative efficiency of 80%.

Detector type	Radionuclide	MDA (Bq/kg)
P type	^{137}Cs	0.6
	^{241}Am	3

4.6.2 MDA Obtained by LS system

The value of the MDA for ^{90}Sr, used in this work, is taken from another reference [40]. In the reference, a detection of *Cerenkov photons* is used to detect the activity of β particles emitted from ^{90}Sr and its daughter nuclide ^{90}Y. The β particles with the minimum energy of 263 keV generate characteristic photons that are seen as blue light, when they travel in water [41]. These photons are called Cerenkov photons, and their blue light can be detected using a LSC. Cerenkov counting requires no scintillation cocktails, and therefore direct counting of a sample dissolved in an aqueous phase is possible. The counting efficiency of Cerenkov photons is lower if the presence of β particles had been detected with the aid of a scintillation cocktail that emits light after being exited by interaction with the particles. However, this is improved as the average energy of β particles increase. Additional advantages, such as no chemical quenching, are given by the counting of Cerenkov photons. In the reference, widely accessible milk (purchased from regular grocery stores) is used to dissolve the radionuclides, instead of water. Therefore, the counting efficiency is strongly affected due to color quenching. This is taken into account by the MDA calculated in the reference. The value of 63.4 Bq/L is given for the MDA of ^{90}Sr dissolved in milk (with 3% fat content) for a counting time of 4 hours [40].

4.6.3 Permissible level of Radionuclide in Food

The activity concentration level of radionuclides in food is regulated by several different organizations worldwide for different purposes. Among them, two of the most commonly referred levels: the Derived Intervention Level (DIL) given from the US Food and Drug Administration (FDA); and the Guideline Level (GL) from the Codex Alimentarius Commission (CAC); are chosen for this work. The DIL is an indication for the necessity of an intervention. When the activity concentration of a radionuclide in food exceeds its DIL, protective measures should be introduced [42] The GL is an indication for acceptance of commodities moving in international trade. When exceeded, governments should make decisions on whether and under what kind of circumstances the food is allowed to be distributed within their countries [43]. The activity concentrations given as the GL and the DIL are shown in **Table 5**. The concentrations are originally given in pCi/L and Bq/kg of readily fed form (in liquid form in the case of IMF) for the GL and DIL, respectively. In **Table 5**, the values are converted to that for IMF in powdered form. The conversion is made based on an assumption that 30 g of IMF dissolved in 200 mL of water gives a volume of 220 mL. The density of IMF in readily fed form (in liquid form) is approximated with that of milk [44].

Table 5: DIL and GL given from FDA and CAC, respectively, are shown for each radionuclide.

Radionuclide	Maximum activity level allowed in IMF (Bq/kg)	
	FDA	CAC
^{90}Sr	1 292	7 67
^{137}Cs	9 689	7 667
^{241}Am	16.44	7.667

5 Scenario Setup

5.1 Radioactive Source

Different types of radioactive sources can be used for an attack such as described in this work. The consequences of the attack, methods to prevent/detect the attack, and counter measures to make the attack more difficult depend, to a large extent, on the type of radioactivity emitted by the sources. Furthermore, the consequences and detectability will, to a large extent, be influenced by the amount of radioactivity involved. It is not possible within the constraints of the current work to consider all possible types of radioactivity. Instead, three different radioactive sources emitting different types of radiation are selected for the scenario where powdered IMF would be contaminated. The amounts of each source are selected based on what could be available to a perpetrator in a realistic scenario:

- ^{90}Sr source in the form of $^{90}SrTiO_3$ with initial activity of the source equivalent to those found in Georgia [15] and current activity as of year 2017 (the source is age of 37 years)
- ^{137}Cs source in the form of $^{137}CsCl$ with current activity of the source equivalent to the Goiânia accident [12] at the time of the accident
- ^{241}Am source in the form of $^{241}AmO_2$ with activity equivalent to 10,000 household smoke detectors as Dhiren Barot intended to use against general public [18]

Characteristics of each radionuclide are shown in **Table 6**.

Table 6: Characteristics of selected radionuclides are shown. For ^{90}Sr and ^{137}Cs, characteristics of their daughter radionuclides ^{90}Y and ^{137m}Ba are included due to their relatively short half-life of 64.0 hours and 2.5 minutes, respectively. ^{241}Am has nine main daughter radionuclides. However, the first daughter ^{237}Np has long half-life of 2.1×10^6 year, and thus characteristics of daughter radionuclides of ^{241}Am are not taken into account above. For β particles, maximum energy is shown.

Radionuclide	Type of radiation; energy (MeV); intensity (%)	Half-life (year)
$^{90}Sr/^{90}Y$	β; 0.546; 100 / β; 2.28; 100	28.8
$^{137}Cs/^{137m}Ba$	β; 0.514; 94 / γ; 0.611; 85	30.1
^{241}Am	α; 5.49; 84.5 and γ; 0.060; 35.9	432.2

Activity of each source is shown in **Table 26** in **Appendix D**. This activity level is hereafter called *selected level*.

Characteristics of each compound are shown in **Table 7**.

Table 7: Characteristics of compounds are shown.

Compound	Physicochemical form	Solubility to water
$^{90}SrTiO_3$	Ceramic [16]	Insoluble
$^{137}CsCl$	Powder [16]	Soluble
$^{241}AmO_2$	Ceramic powder [16]	Insoluble

The ^{241}Am source equipped to household smoke detectors consists of four different layers: a thin layer of Au (2 µm in thickness); a thin layer of Au evenly sintered by AmO_2 in a ceramic powder form (2 µm); another thin layer of Au (2 µm); and a thick layer of Ag (0.2 mm) [45], as shown in **Figure 1**. These four layers are sealed together to form a source. A single source, in the shape of 5 mm diameter disk has a weight of 42.9 mg.

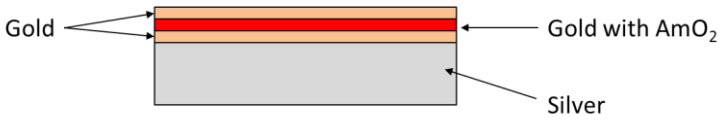

Figure 1: Schematic of ^{241}Am source equipped to a domestic smoke detector is shown.

5.2 Virtual Manufacturing Facility of IMF

A virtual manufacturing facility for production of powdered IMF is established for this work. There are mainly two different manufacturing processes for production of powdered IMF: One is a dry-blending and the other is a wet mixing – spray drying. In the dry-blending process, all of ingredients received at a manufacturing facility are in powdered form. The ingredients are mixed in the facility to meet nutritional requirements of IMF. In the wet mixing – spray drying process, ingredients in both liquid and powder forms are blended together. The mixture is pasteurized, and then sprayed into a dryer to finally produce a powder form [46].

In this facility, the wet blending - spray drying [46, 47] is used. The schematic drawing of the facility is shown in **Figure 2**. Skim milk is delivered using a 30 000 L bulk tank truck. The milk is stored in a 30 000 L storing tank in **Area 1** prior to IMF production. The production begins with four 1 000 L mixing tanks in **Area 2**. 750 L of skim milk and 400 kg of powdered ingredients such as minerals, fats, carbohydrates, stabilizers and emulsifiers are added in each mixing tank. Therefore, one delivery of skim milk results in 40 batches of mixing. All powdered ingredients mentioned above are added at the same time to the skim milk during mixing. From one delivery of skim milk, each tank can produce 10 batches. The mixture is sent to a pasteurization machine and then a homogenization machine. The mixture then enters a 15 000 L storage tank in **Area 3** directly from the homogenization machines. Each storage tank is able to contain the contents of 10 mixing tanks. Hereafter, IMF is produced from one storage tank in **Area 3** at a time. The mixture passes through a dehydration machine followed by a spray drying machine for the mixture to be completely turned into powder. The spray drying process is assumed to take one hour. The powdered IMF is then immediately canned, and each can is labeled with identification numbers including information such as production date and from which specific storage tank in **Area 3** it originates.

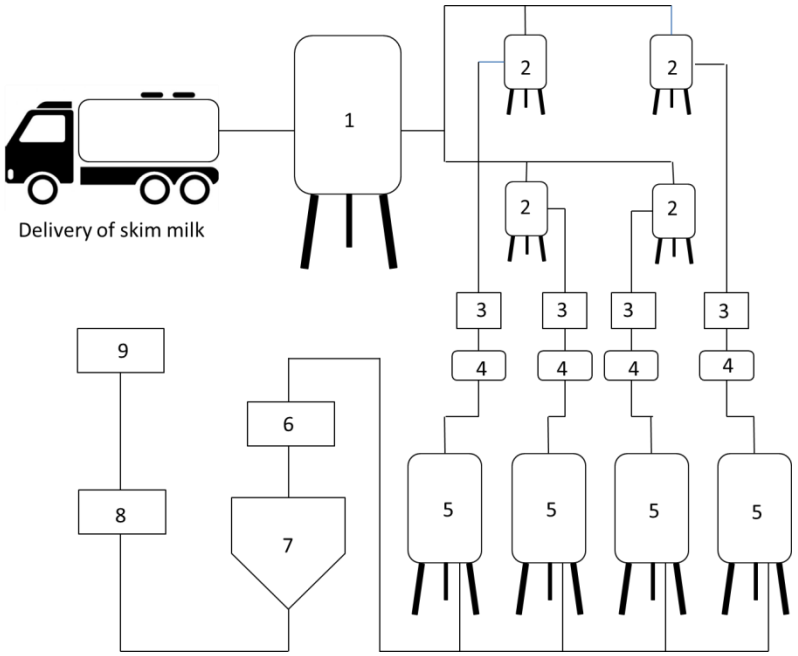

Figure 2: Schematic drawing of a virtual manufacturing facility of powdered IMF is shown. 1) Storing of delivered skim milk. 2) Mixing of powdered ingredients with skim milk. 3) Pasteurization. 4) Homogenization. 5) Storing at lower than 7 °C. 6) Dehydration. 7) Spray drying with inlet air temperature of 180 °C and outlet air temperature of 95 °C. Powder from the dryer is about 30 °C. 8) Sifting for removal of large particles. 9) Packaging using inert gas.

The mass ratio of total solids content (suspended solids and dissolved salts in mixture) [48] to IMF mixture is initially 40% in the mixing process, increases to 55% after the dehydration process, and finally reaches 97% after the spray drying process [46, 47]. This is due to evaporation of water which reduces the weight of water component in the IMF mixture during the production. The mass ratio of total solids content to skim milk is assumed to be 8.9% [44]. The change in the ratio of total solids content to milk/mixture due to change of temperature at each process is neglected. All of the ingredients added to skim milk are assumed to be completely dissolved within the temperature range of operation in the facility. The tanks and machines in the facility are assumed to be tightly connected to each other and sealed during production (except at the time of cleaning of tanks and machines). Each process in the facility is fully automated, and therefore no manual participation by workers of the facility will take place except for cleaning. A worker is placed at each point of manufacturing in order to insure proper functioning of tanks and machines.

The tank of the delivery truck is based on a standard vehicle for delivering milk. The tank has an elliptical cylindrical shape with dimension of 2.8 m in width, 1.8 m in height and 7.6 m in length as shown in **Figure 3**. Distance between a driver and closest surface of the tank is 1.5 m. There are walls of steel exist between the driver and the tank, and the total thickness of those together is assumed to be 1.5 cm. The storage and mixing tanks have a cylindrical shape. Those cylindrical tanks are 3 m by 4.50 m, 1 m by 1.50 m and 2 m by 5 m in diameter and height for the tanks in **Area 1**, **2** and **3**, respectively. All tanks in the facility as well as the tank of delivery truck are made of steel with the thickness of 1.2 mm. During the IMF production, some skim milk and IMF mixture is lost inside the tanks due to residual buildup. The residual levels of milk and mixture remaining in in the tank of the

truck and the storage/mixing tanks in **Area 1**, **2** and **3**, after processing, are estimated to be 30 L, 30 L, 4 L and 20 L, respectively. Loss of milk and mixture inside the pasteurization, homogenization, dehydration and spray drying machines as well as in the pipes that are connected in between them are assumed to be minimal given to the contact surface area compared to the tanks, and therefore neglected. One can of powdered IMF in this facility is set as 800 g. Tin is selected as the material of the can.

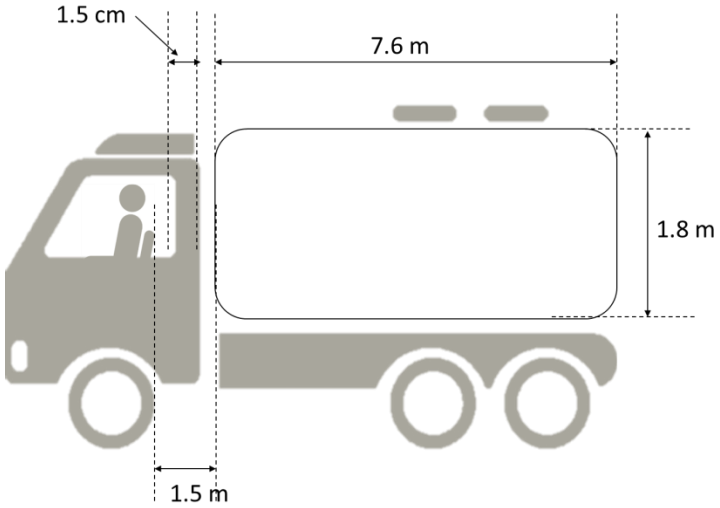

Figure 3: Drawing of tank truck used for the delivery of skim milk is shown. The tank has an elliptical cylindrical shape with dimension of 2.8 m in width, 1.8 m in height and 7.6 m in length. Distance between a driver and the tank is 1.5 m. Within this distance, total 1.5 cm thickness of steel is assumed to exist.

5.3 Model Infant

For the purpose of this work, a model infant is "constructed": The infant is fed only with powdered IMF since birth until it turns 6 months old. Average *daily* serving of powdered IMF is 103.5 g and an average *single* serving is 24.6 g. These assumptions are based on typical feeding tables provided by existing IMF producers [49].

5.4 Contamination Scenarios

Four different scenarios (**Scenario 1, 2, 3** and **4**) are established for contaminating powdered IMF before and during the production, as described in **Appendix D**. **Scenario 4** is inspired by an accidental contamination of powdered IMF with ^{134}Cs and ^{137}Cs in Japan few days after the Fukushima Daiichi Accidents on 11th of March, 2011 [50]. The contaminated powdered IMF was produced between 15th and 20th of March at a facility in city of Kasukabe, 197 km away [51] from the site of the Fukushima Daiichi accident. All of the ingredients used for the production was produced and delivered to the facility before the accident, and therefore it was concluded that radiocesium in air from outside passed through layers of filter, and entered the spray drying machine. Highest concentration of radioactive cesium in the air in the period, when the contamination happened, was 189 Bq/m^3 [52]. This resulted in 30.8 Bq/kg of total radioactive cesium retention to powdered IMF.

For **Scenario 1**, **2** and **3**, the radioactive source is assumed to be evenly distributed in the mixture. For **Scenario 4**, the air containing the source circulates inside the machine, and thus powdered IMF in the

machine is assumed to have equal contact with the source. 5.54% of the source is assumed to be retained to the powdered IMF. The ratio is calculated based on the accidental contamination mentioned above. One type of spray drying machine generates exit air volume of 1.01×10^5 m^3/h at exiting temperature of 110 °C to process 2.50×10^4 kg/h of wet material [53]. The air volume needed in the virtual facility to process one storage tank in **Area 3** (with the IMF mixture of 1.17×10^4 kg) is calculated as 3.44×10^4 m^3 at 6 °C, which was the average daily temperature in the city of Kasukabe in March 2011 [54]. Entered air volume is assumed to be equal to the exit air volume. Assuming that the size of the facility in city of Kasukabe is equal to that of the virtual facility, 6.50×10^6 Bq of radiocesium in the air is calculated to result in retention of 3.60×10^5 Bq to powdered IMF for processing one tank in **Area 3**. This gives the ratio of retained radiocesium to be 5.54%.

In this work, the virtual IMF facility is the only targeted facility, and therefore other contamination methods, such as contamination of powdered ingredients at their manufacturing facilities and contamination of skim milk using contaminated hay to cows, are not considered.

6 Calculation and Result

In this work, all of the calculations have been based on published data, and therefore the precision of calculated results cannot be better than that of the data. The aim of the following calculations is to assess magnitudes, not perform high precision calculations. Therefore, detailed uncertainty calculations are not performed in this work. However, assessments of uncertainty are included in this section as well as in **Section 7**.

Collected parameter values and numbers derived from them were done in an electronic spreadsheet. Due to security concerns, these spreadsheets has been classified according to the Norwegian law about public access to documents (Offentleglova §16), and is therefore not openly available. However, for people with a legitimate need and approval, the spreadsheets are available in electronic form from UiO (Contact person is Prof. Jon Petter Omtvedt, j.p.omtvedt@kjemi.uio.no). Key results from the calculations are assembled in **Appendix D** to this document. However, this appendix is also classified and not distributed together with the main text, which has been written in such a way that is freely available. The classified appendix is only available upon request and after approval, in the same way as the electronic appendix.

6.1 Dilution Rate of Activity at Place in Production Facility

By defining the amount of activity added at the time of contamination to be 100%, the dilution rate of activity in storage/mixing tanks in **Area 1**, **2** and **3** as well as a single can, i.e. the final product which is ready to be distributed, in packaging area are shown in **Table 27** in **Appendix D** for each scenario. Radioactive sources, regardless of their solubility in water, are assumed to be evenly distributed in the tank specified in each scenario, before contaminated milk/mixture is transported to the following machines/tanks. Hereafter, all different concentrations of IMF mixtures from the storage tank in **Area 1** through the spray drying machine are referred to as *mixture*, and powdered IMF as a final product is referred to as *IMF*. The number of cans with contaminated IMF produced is calculated to be 24 125 for **Scenario 1** and 6 031 for **Scenario 2**, **3** and **4**.

6.2 Health Effects Caused by Selected Sources

The amount of the selected radionuclides left in a single can is shown in **Table 28** in **Appendix D** for each scenario. This is when the activity at the time of contamination is at the selected level (shown in **Table 26** in **Appendix D**).

For mortality, hematopoietic syndrome and gastrointestinal syndrome are the most lethal syndromes after ingestion of a radionuclide. Target organs for hematopoietic and gastrointestinal syndrome are the bone marrow and the large intestine, respectively. In order to determine a dominancy of the syndromes for each source, the *syndrome coefficient* is introduced. The syndrome coefficient is defined as a sum of absorbed dose-rate coefficient for ingestion to target organs of an infant from day 1 (the day of ingestion) until the day specified, divided by the threshold of corresponding syndrome. The coefficient is given with the unit of per Bq per day. The greater the coefficient, the more the corresponding syndrome dominates with the given activity of a radionuclide. **Figure 4**

shows the syndrome coefficient as a function of days since ingestion for each radionuclide. The threshold of hematopoietic and gastrointestinal syndrome is 1.5 Gy (without medical treatment) and 23 Gy, respectively [33]. The thresholds are based on the syndromes to occur in 1% of adults. The ingestion is assumed to occur only on day 1. From **Figure 4**, hematopoietic syndrome dominates for ingestion of ^{137}Cs to an infant regardless to activity ingested. For ^{90}Sr and ^{241}Am, gastrointestinal syndrome dominates for the first 3 days and 4 days, respectively, and hematopoietic syndrome dominates thereafter. This means that, if the activity ingested on day 1 is small enough not to reach the threshold of gastrointestinal syndrome during its dominancy, hematopoietic syndrome is the only cause of concern for mortality in the case of ^{90}Sr and ^{241}Am. The upper limit of activity on day 1 not to cause gastrointestinal syndrome during its dominancy is calculated as 5.05×10^{5} Bq and 3.21×10^{5} Bq for ^{90}Sr and ^{241}Am, respectively. Therefore, as long as radionuclides ingested on day 1 is below the calculated activities and no additional ingestions occurs after day 2, hematopoietic syndrome dominates for all of the radionuclides.

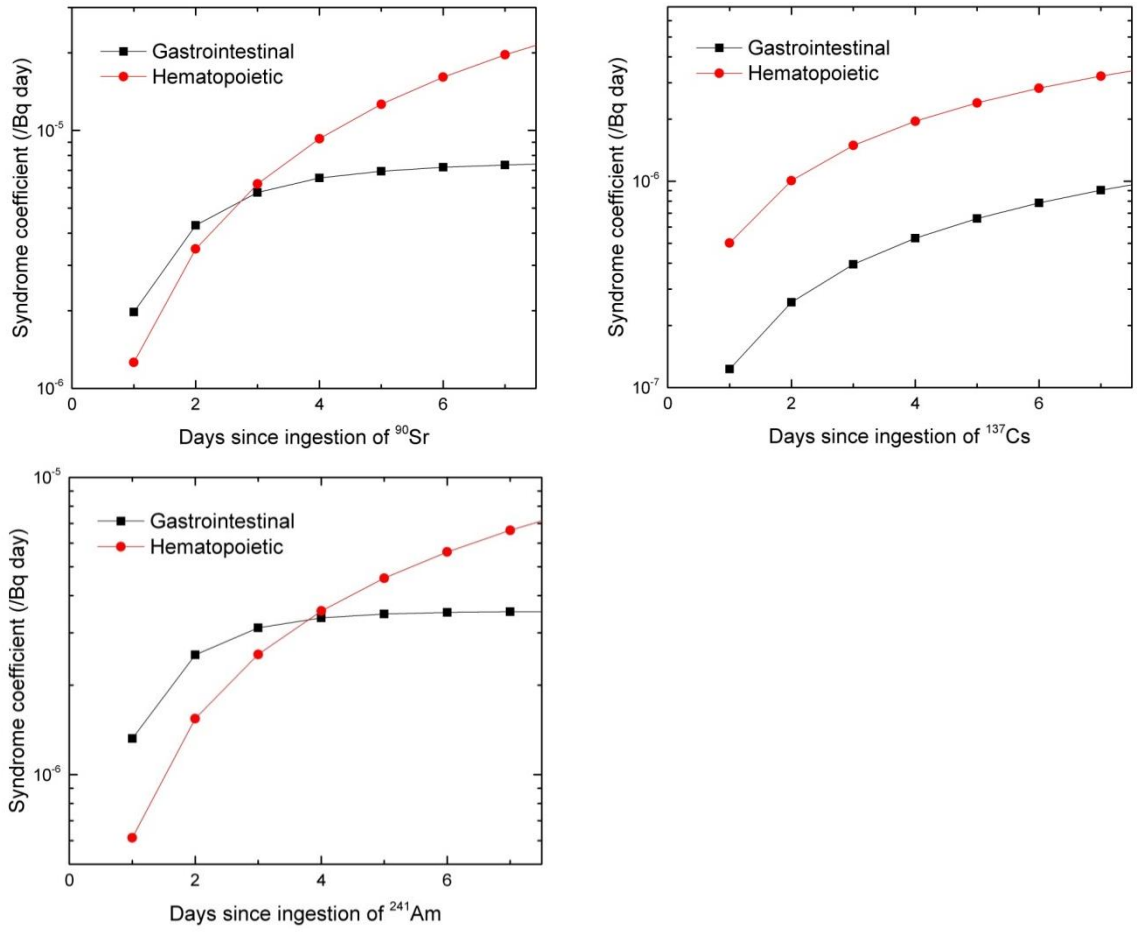

Figure 4: Syndrome coefficient in /Bq·day of hematopoietic and gastrointestinal syndromes is shown as a function of days since ingestion of each radionuclide.

Absorbed dose on day 1, to targeted organs of an infant by a *single* serving of IMF (24.6 g) from a can containing ^{90}Sr and ^{137}Cs with the activity at selected level, as specified in **Table 28**, is shown in **Table 29** in **Appendix D**. The single serving is chosen for these two sources, since the absorbed dose

received from the serving is calculated to give results far beyond the threshold of prodromal syndrome for ingestion of radionuclides. Symptoms of the prodromal syndrome, vomiting and diarrhea, are assumed to appear when the absorbed dose to the abdomen of the infant reaches the threshold of the syndrome. Therefore, the infant is assumed to no longer be fed with the same IMF. The threshold for prodromal syndrome is based on the syndrome to occur with a 50% risk in an adult. For ^{90}Sr, the large intestine is the organ of interest since the activity ingested from a single serving is above 5.05×10^{5} Bq for all scenarios. For ^{137}Cs, the bone marrow is the organ of interest since the hematopoietic syndrome always dominates for the radionuclide.

For ^{241}Am with the activity at the selected level, as specified in **Table 28**, the absorbed dose to abdomen of an infant reaches the threshold of prodromal syndrome on day 4 for **Scenario 1** and day 2 for **Scenario 2** and **3**, assuming that contaminated IMF is *consecutively* fed; that is, 24.6 g per serving and on average 4.2 times per day. For **Scenario 4**, the absorbed dose received from being fed a whole can of contaminated IMF is still below the threshold on day 8, when the entire can has been finished. In case of ^{241}Am, the activity ingested from a single serving is far below 3.21×10^{5} Bq in any scenario. Therefore, hematopoietic syndrome dominates for the source with the activity at selected level. By assuming that the infant is no longer being fed with the same IMF as soon as the symptoms for prodromal syndrome appear, the absorbed dose received in the bone marrow of the infant, from consecutive serving for days mentioned above, is shown in **Figure 5** for each scenario as a function of days since the first ingestion of the radionuclide.

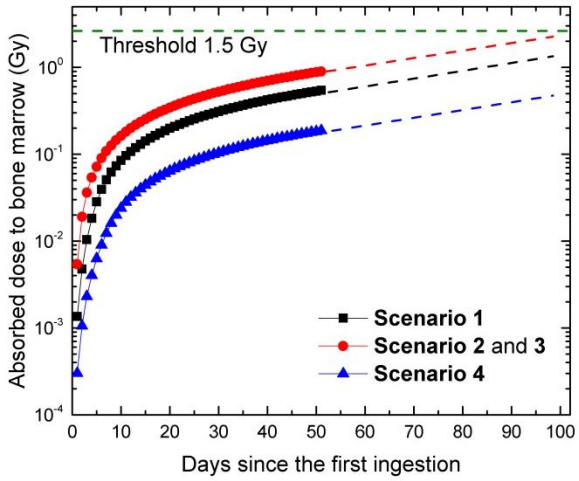

Figure 5: Absorbed dose given to the bone marrow of an infant by being fed ^{241}Am-contaminated IMF with the activity at selected level, as specified in **Table 28**, is shown. The absorbed dose is received from 5, 2 and 8 days of consecutive feeding for **Scenario 1**, **2** and **3** and **4**, respectively. A whole can is equivalent to 7.7 of daily servings. The dashed line for each scenario shows the total absorbed dose assumed after the first 50 days. The dashed line in green shows the threshold of hematopoietic syndrome.

6.3 Necessary Activity to Cause Deterministic Effects

The necessary activity in a can, for a *single* serving of IMF to give the absorbed dose which reaches the threshold of mortality on day 7, is investigated as an example of the activity causing mortality to an infant. Hereafter, this activity level is called *mortality level*. For the threshold to be reached on Day 7 for the first time, hematopoietic syndrome must dominate. The rationale for the necessary

activity to be based on a single serving is due to immediate development of prodromal syndrome from the serving. A period of 7 days is chosen, for the absorbed dose to reach the threshold, in order for the contaminated IMF to be distributed widely before the contamination event to the IMF is discovered. The necessary activity in a can of IMF for the mortality level is shown in **Table 30** in **Appendix D** for the radionuclides previously selected. However, the symptoms for prodromal syndrome may be confused with other common illnesses. Therefore, the infants, who are fed with more than a single serving of contaminated IMF with the activity specified in **Table 30**, will receive a total absorbed dose that reaches the threshold of hematopoietic syndrome earlier than day 7.

Necessary activity in a can, for a single serving of IMF to give the absorbed dose which reaches the threshold of morbidity on day 7, is also investigated as an example of the activity causing morbidity to an infant. Hereafter, this activity level is called *morbidity level*. The necessary activity in a can for the morbidity level is shown in **Table 31** in **Appendix D** for the radionuclides. Infants who are fed with more than a single serving of contaminated IMF, with the activity specified in **Table 31**, will receive the total absorbed dose which reaches the threshold of prodromal syndromes earlier than day 7. The absorbed dose may eventually reach the threshold of hematopoietic syndrome, if the infants are given consecutive servings. In the case of the ^{90}Sr source, the necessary activity would become less to cause mortality and morbidity, if the source is sufficiently aged. This is due to a secular equilibrium of ^{90}Sr and ^{90}Y. The absorbed dose rate coefficient used in the calculation takes into account ^{90}Y that are generated after ingestion of ^{90}Sr, but not before. The selected ^{90}Sr source is age of 37 years, and the activity of ^{90}Y in the source is calculated to be 8 orders of magnitude smaller than that of ^{90}Sr. The magnitudes in effect on the necessary activity at mortality and morbidity level, due to ingestion of ^{90}Y coexisting with ^{90}Sr, is not investigated in this work.

Based on **Table 30** and **31**, the necessary activity at the time of contamination to reach the mortality and morbidity level in each scenario is shown in **Table 32** in **Appendix D**.

6.4 Count Rate Measured from a can of contaminated IMF

In order to calculate a count rate measured from a can of contaminated IMF, γ rays are of interest for ^{137}Cs and ^{241}Am sources, while β particles are relevant for a ^{90}Sr source. As for the material of the can, aluminum and tin are the commonly used. However, in order to calculate the count rate of γ rays and β particles conservatively, tin is selected for all of the sources. Tin absorbs energy of γ rays and β particles more than aluminum due to its higher density. In the calculation, the mass absorption coefficient and the stopping power of IMF is approximated with those of lithium, due to their similar density: the density of IMF and lithium is 0.561 g/cm^3 [55] and 0.534 g/cm^3 [56], respectively. As a detector, a NaI(Tl) detector with crystal size of 7.62 cm diameter and length of 7.62 cm (3 inches by 3 inches) is assumed to be used.

6.4.1 Count Rate of γ Rays

Approximations and assumptions used in the calculation of the count rate of γ rays, emitted from a can of contaminated IMF with ^{137}Cs and ^{241}Am sources, are schematically shown in **Figure 6**. The can is divided in layers that are 0.5 cm in thickness. Each layer is parallel to the detector surface area. The radionuclide in each layer is assumed to be placed in the middle of the layer as a point source. Five

different detection distances, 0.5 cm, 2 cm, 5 cm, 10 cm, 25 cm and 50 cm, are chosen between the detector surface area and the closest part of the can. No other material except air is assumed to exist within the distance. Intensity of the γ rays lost due to interaction with IMF, tin layer, and air within the corresponding detection distance is taken into account. The geometry between the point source in each layer and the detector surface area is also taken into account. The interaction between the detector crystal and the γ rays that reach the detector are assumed to occur with 100% efficiency.

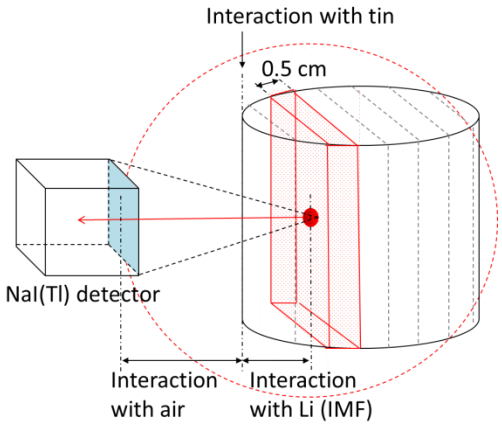

Figure 6: Approximations and assumptions used in the calculation of the count rate of γ rays emitted from a can of IMF contaminated with ^{137}Cs and ^{241}Am sources. The colored volume represents one of virtual layers. Within the layer, a radionuclide is, in reality, evenly distributed. However, this radionuclide is assumed to be collected in the middle of the layer as a point source, which is represented by a red dot. γ rays that reach the detector surface after penetrating the IMF, the tin and the air is represented by a red arrow. A dashed line in red shows a sphere with the radius being the distance between the point source and the farthest part of the detector surface area. This sphere represents that γ ray from the point source are isotropically emitted. However, only the γ rays that are emitted to the area of the sphere which overlaps with the detector surface area give count rate. The detector surface area is colored in blue.

The count rates of the γ rays emitted from the can of IMF contaminated with ^{137}Cs and ^{241}Am sources are shown in **Table 8** and **9**, respectively, in different detection distance and at different activity levels. Activity in a can of IMF at each level (selected, mortality and morbidity) is specified in **Table 28**, **30** and **31**.

Table 8: Count rates in cps of the γ rays emitted from a can of IMF contaminated with ^{137}Cs source, are shown in different detection distance and each activity level.

Count rate (cps) of γ rays emitted from ^{137}Cs sources at detection distance (cm)							
		0.5	**2**	**5**	**10**	**25**	**50**
Selected level	**Scenario 1**	1.36×10^{8}	9.00×10^{7}	4.76×10^{7}	2.25×10^{7}	6.00×10^{6}	1.83×10^{6}
	Scenario 2	5.47×10^{8}	3.61×10^{8}	1.91×10^{8}	9.02×10^{7}	2.40×10^{7}	7.37×10^{6}
	Scenario 3	5.49×10^{8}	3.62×10^{8}	1.92×10^{8}	9.06×10^{7}	2.41×10^{7}	7.39×10^{6}
	Scenario 4	3.03×10^{7}	2.00×10^{7}	1.06×10^{7}	5.00×10^{6}	1.33×10^{6}	4.09×10^{5}
Mortality level		8.76×10^{5}	5.78×10^{5}	3.06×10^{5}	1.45×10^{5}	3.85×10^{4}	1.18×10^{4}
Morbidity level		3.98×10^{4}	2.63×10^{4}	1.39×10^{4}	6.57×10^{3}	1.75×10^{3}	5.36×10^{2}

Table 9: Count rates in cps of the γ rays emitted from a can of IMF contaminated with ^{241}Am source, are shown in different detection distance and each activity level.

		Count rate (cps) of γ rays from ^{241}Am sources at detection distance (cm)					
		0.5	**2**	**5**	**10**	**25**	**50**
Selected level	**Scenario 1**	3.09×10^{2}	2.04×10^{2}	1.08×10^{2}	50.93	13.57	4.16
	Scenario 2	1.24×10^{3}	8.17×10^{2}	4.32×10^{2}	2.04×10^{2}	54.38	16.66
	Scenario 3	1.24×10^{3}	8.20×10^{2}	4.34×10^{2}	2.05×10^{2}	54.60	16.73
	Scenario 4	68.62	45.30	23.96	11.32	3.02	0.925
Mortality level		1.33×10^{5}	8.78×10^{4}	4.65×10^{4}	2.20×10^{4}	5.85×10^{3}	1.79×10^{3}
Morbidity level		5.09×10^{3}	3.36×10^{3}	1.78×10^{3}	8.40×10^{2}	2.24×10^{2}	68.60

6.4.2 Count Rate of β particles

A ^{90}Sr source emits β particles from both ^{90}Sr and its daughter radionuclide ^{90}Y. However, a β particle emitted from ^{90}Sr, with its average energy assumed to be 182 keV, i.e. one-third of the maximum energy of the β particles emitted from ^{90}Sr, loses its entire energy interacting with the tin layer. Therefore, the count rate of the β particles emitted from ^{90}Sr is neglected in the calculation, and thus that of the β particles emitted from ^{90}Y is only of interest in this calculation. Approximations and assumptions used for the calculation are schematically shown in **Figure 7, 8** and **9**. In the calculation, all of the β particles emitted from ^{90}Y is assumed to have the average energy of 760 keV.

Majority of the β particles emitted from ^{90}Y inside the can lose their total energies to IMF before reaching the tin layer. Therefore, an approximation is made in order to determine a volume in which the β particles emitted from ^{90}Y have a potential to pass through the tin layer. This volume is shown in **Figure 7**.

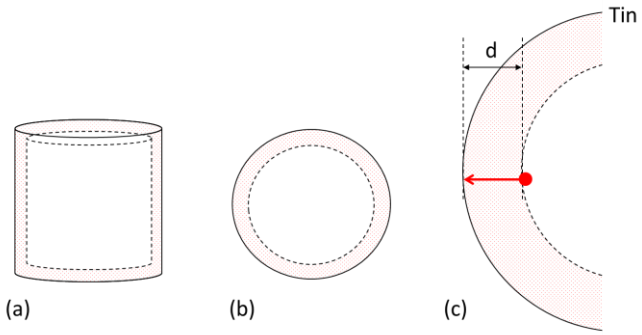

Figure 7: Approximation used in order to determine the colored volume in which the β particles emitted from ^{90}Y have a potential to pass through a tin layer. (a) The volume is seen from the side of the can. (b) The volume is seen from the top of the can. (c) Thickness of the volume *d* as seen from the top of the can. The red dot represents a β particle with the average energy of 760 keV. The red arrow represents the path of the β particle.

Thickness of the specified volume, shown as *d*, is defined to be the minimum thickness of IMF that the β particles, emitted from ^{90}Y with average energy, lose their total energy by interacting with both IMF of the thickness *d* and the tin layer of the thickness 0.2 mm. Therefore, the β particles emitted

outside the volume is assumed not to pass through the tin layer. The thickness *d* is calculated as 0.62 cm. The specified volume is calculated to be 25.6% of the entire volume of IMF in the can.

^{90}Y inside the specified volume emits β particles isotropically. Thus, another approximation is necessary in order to determine the fraction of the β particles that are emitted toward the tin layer. For this approximation, a β particle is placed in the middle of the specified volume, i.e. at the thickness of $\frac{1}{2}d$, as shown in **Figure 8**. As seen in **Figure 8** (a), the angle of emission of the β particle which passes through the tin layer is calculated to be 120°. The corresponding solid angle to 120° is π sr. Thus, 25% of the β particles emitted from the middle of the specified volume is assumed to pass through the tin layer. However, this approximation involves large uncertainties on both the upper and the lower side. The uncertainty pertaining to the lower side is that some β particles that manage to pass through the tin layer lose a vast majority of their energies interacting with IMF and the tin, before passing through the layer. Therefore, the β particles may lose the rest of their energy to air while flying toward the detector. Or, the energy conserved to the particles when reaching the detector crystal, may not be sufficiently large enough to generate a signal, i.e. count rate.

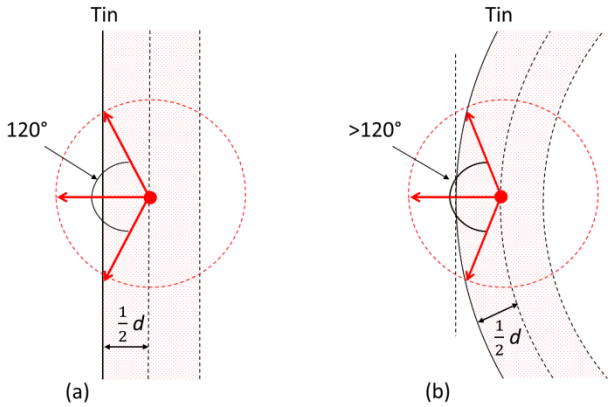

Figure 8: Approximation used in order to determine a fraction of β particles that are emitted toward and pass through the tin layer. β particle with average energy of 760 keV is placed in the middle of the volume, which is specified in **Figure 7**. (a) A view from the side of a can. (b) A view from the top of a can. The red dot represents the origin of a β particle with the average energy of 760 keV. The red arrow represents the path of the β particle. A dashed line in red shows a sphere with the radius being *d*. This sphere represents that the β particle is isotropically emitted from its origin.

The uncertainty pertaining to the upper side is that a part of the specified volume is bent, as shown in **Figure 8** (b). This gives a slightly greater angle to the emission of the β particles that pass through the tin layer, than the angle calculated based on **Figure 8** (a). Therefore, in this work, the uncertainty of the fraction of β particles to pass through the tin layer is assumed to be ±15%.

Finally, an approximation used to calculate the count rate of the β particles that have passed through the tin layer is shown in **Figure 9**.

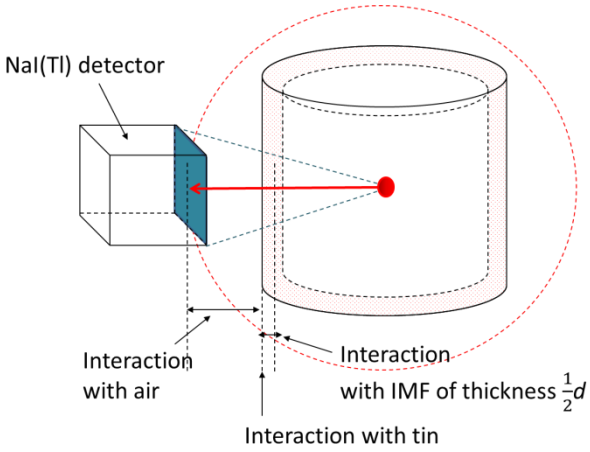

Figure 9: Approximation used in order to calculate the count rate of the β particles that have passed through the tin layer. The β particles originate from the middle of the can, as a point source.

The fraction of β particles that pass through the tin layer, i.e. 25% of the β particles emitted from the specified volume, is now assumed to originate from the middle of the can, as a point source. Detection distances of 0.5 cm, 2 cm, 5 cm, 10 cm, 25 cm and 50 cm are chosen. No other material except air is assumed to exist within the distance. Between the point source and the detector surface area, the energies of the β particles lost due to interaction with IMF of thickness $\frac{1}{2}d$, the tin layer and the air within the corresponding detection distance are taken into account. The geometry between the point source and the detector surface area is also taken into account. The interaction between the detector crystal and the β particles are assumed to occur with 100% efficiency. The count rate of the β particles, emitted from a can of IMF contaminated with ^{90}Sr source, is shown in **Table 10** in different detection distance and at different activity level. The energy of the β particles when reaching the detector surface area is calculated to be 321 keV, 317 keV, 310 keV, 297 keV, 261 keV and 200 keV for the detection distance of 0.5 cm, 2 cm, 5 cm, 10 cm, 25 cm and 50 cm, respectively.

Table 10: Count rates in cps of the β particles emitted from a can of IMF contaminated with ^{90}Sr source, are shown in different detection distance and at different activity level.

Count rate (cps) of β particles emitted from ^{90}Sr sources at detection distance (cm)							
		0.5	**2**	**5**	**10**	**25**	**50**
Selected level	**Scenario 1**	1.15×10^{8}	7.56×10^{7}	4.00×10^{7}	1.89×10^{7}	5.03×10^{6}	1.54×10^{6}
	Scenario 2	4.59×10^{8}	3.03×10^{8}	1.60×10^{8}	7.57×10^{7}	2.02×10^{7}	6.18×10^{6}
	Scenario 3	4.61×10^{8}	3.04×10^{8}	1.61×10^{8}	7.60×10^{7}	2.03×10^{7}	6.21×10^{6}
	Scenario 4	2.55×10^{7}	1.68×10^{7}	8.89×10^{6}	4.20×10^{6}	1.12×10^{6}	3.43×10^{5}
Mortality level		1.16×10^{4}	7.66×10^{3}	4.05×10^{3}	1.91×10^{3}	5.10×10^{2}	1.56×10^{2}
Morbidity level		6.40×10^{2}	4.23×10^{2}	2.24×10^{2}	1.06×10^{2}	28.15	8.63

As mentioned above, the uncertainty of the fraction of β particles, emitted from the specified volume and pass through the tin layer, is ±15%. This propagates to an uncertainty of ±60% in the calculated values.

6.5 Deterministic Effects on Workers

Workers in the facility may be exposed to external radiation emitted from the respective sources inside the tanks in the facility. For ^{137}Cs and ^{241}Am, the external dose will be induced by the respective γ-rays emissions. For the ^{90}Sr source, bremsstrahlung photons will be generated due to β particle interaction with the steel walls of each tank as well as the mixture inside. Bremsstrahlung photons generated from the β particles emitted from ^{90}Sr are neglected. This is because generation of bremsstrahlung photons becomes more intense as the kinetic energy of the β particle increases. Therefore, to simplify the calculations, only β particles from the daughter radionuclide ^{90}Y are considered here. No other radiation will escape the tanks since neither the β particles emitted from ^{90}Sr, ^{90}Y and ^{137}Cs or the α particles emitted from ^{241}Am are capable of passing through the steel wall that is assumed to have a thickness of 1.2 mm. For the calculations, the workers are placed 50 cm away from the closest surface of a given tank.

6.5.1 Absorbed Dose Rate from γ Rays

Approximations and assumptions used in the calculation of the absorbed dose rate, given from the external exposure to the γ rays emitted from ^{137}Cs and ^{241}Am inside a tank truck, are shown in **Figure 10**.

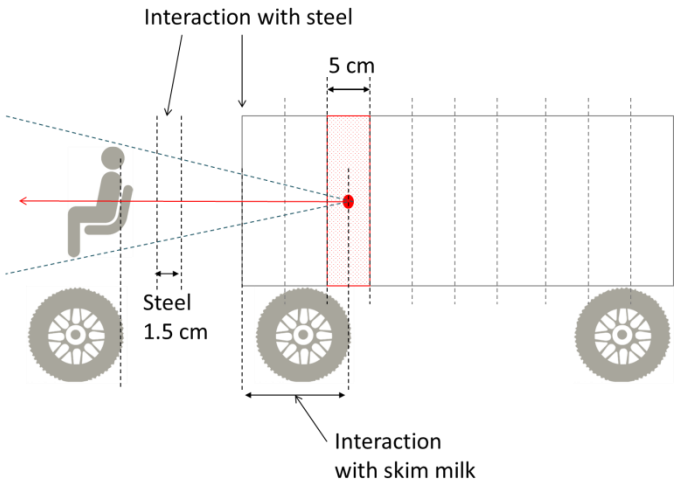

Figure 10: Approximations and assumptions used in the calculation of the absorbed dose rate, given from the external exposure to the γ rays emitted from ^{137}Cs and ^{241}Am inside a tank truck, is shown. The colored volume represents one of the layers. Within the layer, a radionuclide is assumed to be collected as a point source, which is represented by a red dot. The γ rays, giving an absorbed dose to a driver after penetrating the skim milk and the steels, are represented by a red arrow.

The tank is divided in layers that are 5 cm in thickness. Each layer is parallel to the driver. The radionuclide in each layer is assumed to be placed in the middle of the layer, as a point source. The intensity of the γ rays lost due to attenuation with the skim milk; the steel wall of the tank; and the steel walls of 1.5 cm thickness between the driver and the tank, are taken into account. The intensity of the γ rays lost due to attenuation with the air between the tank and the driver is neglected. The geometry between the point source in each layer and the driver is taken into account by the given

absorbed dose rate coefficient for external exposure, prior to the calculation. Mass absorption coefficients of skim milk and steel are approximated with those of water and iron, respectively.

Approximations and assumptions used in the calculation of the absorbed dose rate, given from the external exposure to the γ rays emitted from ^{137}Cs and ^{241}Am inside the storage/mixing tanks in **Area 1**, **2** and **3**, are shown in **Figure 11**.

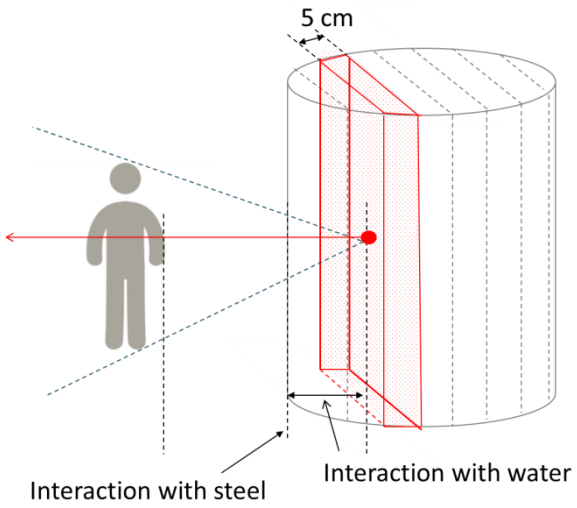

Figure 11: Approximations and assumptions used in the calculation of the absorbed dose rate, given from the external exposure to the γ rays emitted from ^{137}Cs and ^{241}Am inside the storage/mixing tanks in **Area 1**, **2** and **3**, is shown. The colored volume represents one of the layers. The radionuclide is assumed to be collected as a point source, which is represented by a red dot. The γ rays, giving an absorbed dose to a driver after penetrating the mixture and the steel layer, are represented by a red arrow.

A tank is divided in layers that are 5 cm in thickness. Each layer is parallel to the worker who receives external exposure of γ rays. No other material except air is assumed to exist in between the worker and the tank. The radionuclide in each layer is assumed to be placed in the middle of the layer, as a point source. The intensity of the γ rays lost due to interaction with the mixture and the steel layer is taken into account. The intensity of the γ rays lost due to attenuation with the air between the tank and the worker is neglected. Mass absorption coefficient of the mixture is approximated with that of water.

The absorbed dose rates that are externally given to a worker, from the γ rays emitted from ^{137}Cs and ^{241}Am inside the tank of the tank truck, as well as from the storage/mixing tanks in **Area 1**, **2** and **3**, are shown in **Table 11** and **12** for ^{137}Cs and ^{241}Am, respectively, in each scenario and activity level.

Table 11: External absorbed dose rates in Gy/h that would be received by a worker from γ rays emitted from a ^{137}Cs for the different scenario is shown.

Scenario	Activity level	Absorbed dose rate (Gy/h) given from γ rays of ^{137}Cs			
		Delivery	Area 1	Area 2	Area 3
1	Selected	1.1×10^{-2}	0.17	2.1×10^{-2}	7.5×10^{-2}
	Mortality	5.2×10^{-5}	8.0×10^{-4}	9.9×10^{-5}	3.6×10^{-4}
	Morbidity	2.3×10^{-6}	3.6×10^{-5}	4.5×10^{-6}	1.6×10^{-5}
2	Selected			0.83	0.30
	Mortality			9.9×10^{-4}	3.6×10^{-4}
	Morbidity			4.5×10^{-5}	1.6×10^{-5}
3	Selected				0.30
	Mortality				3.6×10^{-4}
	Morbidity				1.6×10^{-5}

Table 12: External absorbed dose rates in Gy/h that would be received by a worker from γ rays emitted from a ^{137}Cs for the different scenario is shown. For the tank of the tank truck, the γ rays are fully absorbed by the steel walls of total 1.5 cm thickness existing between the driver and the tank, and thus no absorbed dose rate is given to the driver.

Scenario	Activity level	Absorbed dose rate (Gy/h) given from γ rays of ^{241}Am			
		Delivery	Area 1	Area 2	Area 3
1	Selected	0	3.3×10^{-8}	4.2×10^{-9}	1.5×10^{-8}
	Mortality	0	1.0×10^{-5}	1.3×10^{-6}	4.8×10^{-6}
	Morbidity	0	4.0×10^{-7}	5.1×10^{-8}	1.8×10^{-7}
2	Selected			1.7×10^{-7}	5.9×10^{-8}
	Mortality			1.3×10^{-5}	4.8×10^{-6}
	Morbidity			5.1×10^{-7}	1.8×10^{-7}
3	Selected				6.0×10^{-8}
	Mortality				4.8×10^{-6}
	Morbidity				1.8×10^{-7}

6.5.2 Absorbed Dose Rate from Bremsstrahlung

In order to calculate the amount of bremsstrahlung photons generated from the β particles emitted from ^{90}Y, an average energy of 760 keV is assumed for all the β particles. Two separated calculations are made in order to calculate the absorbed dose rate from the bremsstrahlung photons: the bremsstrahlung photons generated in the mixture inside each tank; and the bremsstrahlung photons generated in the steel layer of each tank.

In the calculation of the bremsstrahlung photons generated in the mixture, all of the β particles emitted inside each tank are considered. The total energy emitted from the β particles is assumed to be fully absorbed by the mixture. Therefore, radiation yield corresponding to a β particle with the energy of 760 keV is used to calculate the fraction of the β particle energy converted into

bremsstrahlung photons. The average energy of the bremsstrahlung photons is assumed to be 50 keV. This is the energy of bremsstrahlung photons with the highest intensity that are generated from the β particles of ^{90}Sr and ^{90}Y in materials with different densities [57, 58]. Each tank is divided into layers with the thickness of 5 cm, as shown in **Figure 11**. The bremsstrahlung photons generated in each layer is assumed to originate in a point source, which is placed in the middle of the layer. The interaction of the bremsstrahlung photons with the mixture of corresponding thickness and the steel layer of each tank are taken into account. Bremsstrahlung photons have an angular dependency in its emitted direction. However, the β particles are emitted isotropically, and therefore the bremsstrahlung is assumed to be emitted also isotropically from the point source. The absorbed dose rate coefficient of the bremsstrahlung photons is approximated with that of ^{156m}Tb, due to the properties of this radionuclide: ^{156m}Tb disintegrates via internal transition. The only γ rays emitted through the disintegration have the energy of 49.6 keV and the intensity of 74%.

In the calculation of the bremsstrahlung photons generated in the steel layer of each tank, a fraction of the β particles that have a potential to reach the steel layer is approximated. A specific volume of the mixture in each tank is determined in the similar way as shown in **Figure 7**. The thickness of the specified volume d_{Brem} is defined to be the minimum thickness of the mixture between the steel layer and the origin of a β particle. The β particle, emitted perpendicularly to the steel layer, loses its total energy by interacting with the mixture before reaching the steel layer. The β particles emitted outside the specified volume is assumed not to interact with the steel layer. The distance d_{Brem} is calculated to be 4.0 mm. The specified volume is calculated to be 0.071%, 0.217% and 0.096% of the entire volume of the mixture in the storage/mixing tanks in **Area 1**, **2** and **3**, respectively. The radiation yield corresponding to a β particle with the energy of 381 keV is used to calculate the fraction of the β particle energy converted into bremsstrahlung photons. This is the energy of the β particle when it interacts with the mixture with thickness of $\frac{1}{2}d_{\text{Brem}}$ and reaches the steel layer. This is based on an assumption that all of the β particles in the specified volume are emitted from the middle of the volume. The radiation yield from the steel is approximated with that of iron. ^{90}Y inside the specified volume emits β particles isotropically. Thus, another approximation, in the same way as shown in **Figure 8** (a), is necessary in order to determine the fraction of the β particles that are emitted toward the steel layer and interact with it. The angle of emission of the β particles which interact with the steel layer is calculated to be also 120°, and therefore the corresponding solid angle is π sr. Thus, 25% of the β particles in the specified volume are assumed to interact with the steel layer. However, this approximation also involves large uncertainty on the upper side, as shown in **Figure 8** (b). The lower side of the uncertainty is neglected since intensity of photons lost due to interaction with air is far less significant compared to that of β particles. Therefore, in order to calculate the absorbed dose rate given from the bremsstrahlung photons conservatively, i.e. to overestimate in this case, the upper side of the uncertainty, as assumed earlier as +15%, is taken into account by the calculation: the fraction of β particles interacting with the steel layer is now modified to 40% from 25%.

Finally, the bremsstrahlung photons with the energy of 50 keV is assumed to originate in the middle of each tank, as a point source, as shown in **Figure 12**. The bremsstrahlung photons are assumed to be emitted isotropically from the point source.

The total absorbed dose rates that are externally given to a worker, from the bremsstrahlung photons from the tank of the tank truck as well as from the storage/mixing tanks in **Area 1**, **2** and **3** are shown in **Table 13** in each scenario and at each activity level.

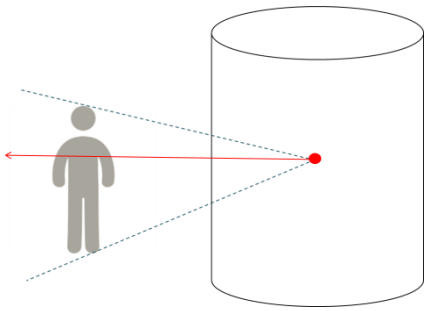

Figure 12: Approximation used in the calculation of the absorbed dose rate, given from external exposure to the bremsstrahlung photons generated in the steel layer of each tank, is shown. The bremsstrahlung photons are assumed to originate in the middle of the tank as a point source, which is represented by a red dot. The bremsstrahlung photons, giving an absorbed dose to a worker, are represented by a red arrow.

Table 13: Absorbed dose rate in Gy/h that is externally given to the worker from the bremsstrahlung photons from the tank in each production area is shown in each scenario and at each activity level. Only the bremsstrahlung photons generated by the β particles emitted from ^{90}Y is calculated. The bremsstrahlung photons generated from both the mixture and the steel layer is taken into account. No absorbed dose rate is given to the driver of the tank truck since the photon energy of 50 keV is fully absorbed by the steel layer of 1.5 cm thickness that is placed between the driver and the tank.

Scenario	Activity level	Absorbed dose rate (Gy/h) given from bremsstrahlung originate in ^{90}Y			
		Delivery	Area 1	Area 2	Area 3
1	Selected	0	3.8×10^{-4}	5.6×10^{-5}	1.8×10^{-4}
	Mortality	0	2.9×10^{-8}	4.3×10^{-9}	1.2×10^{-8}
	Morbidity	0	1.6×10^{-9}	2.4×10^{-10}	2.2×10^{-9}
2	Selected			2.3×10^{-3}	7.2×10^{-4}
	Mortality			4.3×10^{-8}	1.2×10^{-8}
	Morbidity			2.4×10^{-9}	2.2×10^{-9}
3	Selected				7.2×10^{-4}
	Mortality				1.2×10^{-8}
	Morbidity				2.2×10^{-9}

The absorbed dose rates, given from the bremsstrahlung photons generated from the mixture in the storage/mixing tanks in **Area 1**, **2** and **3**, are 88%, 76% and 85% of the total absorbed dose rates shown in **Table 13**, respectively.

6.6 Temperature Increase

The rate of temperature increase of the mixture and IMF, due to disintegration of the radionuclides is shown in **Table 14**, **15** and **16** for ^{90}Sr/^{90}Y, ^{137}Cs and ^{241}Am, respectively, at each place in the

production facility, in each scenario and at each activity level. The heat generation contributed by ^{90}Y is taken into account to the given value of specific power [34]. The mass ratio of total solids content to milk/mixture at each place in the production facility is also taken into account. The specific heat of solid compounds in the mixture as well as IMF is approximated with 0.36 cal/g·°C, which is the specific heat of dry non-fat milk powder [37].

Table 14: Rate of temperature increase of the mixture and IMF, due to disintegration of ^{90}Sr and ^{90}Y is shown in each production area, in each scenario and at each activity level.

Scenario	Activity level	Rate of temperature increase (°C/day) due to $^{90}Sr/^{90}Y$			
		Area 1	Area 2	Area 3	Packaging
1	Selected	3.6×10^{-2}	3.0×10^{-2}	3.0×10^{-2}	0.14
	Mortality	2.7×10^{-6}	2.3×10^{-6}	2.3×10^{-6}	1.1×10^{-5}
	Morbidity	1.5×10^{-7}	1.2×10^{-7}	1.2×10^{-7}	5.9×10^{-7}
2	Selected		1.2	0.12	0.56
	Mortality		2.2×10^{-5}	2.2×10^{-6}	1.1×10^{-5}
	Morbidity		1.2×10^{-6}	1.2×10^{-7}	5.9×10^{-7}
3	Selected			0.12	0.56
	Mortality			2.2×10^{-6}	1.1×10^{-5}
	Morbidity			1.2×10^{-7}	5.9×10^{-7}
4	Selected				3.1×10^{-2}
	Mortality				1.1×10^{-5}
	Morbidity				5.9×10^{-7}

Table 15: Rate of temperature increase of the mixture and IMF, due to disintegration of ^{137}Cs is shown at each production area, in each scenario and at each activity level.

Scenario	Activity level	Rate of temperature increase (°C/day) due to ^{137}Cs			
		Area 1	Area 2	Area 3	Packaging
1	Selected	2.7×10^{-3}	2.2×10^{-3}	2.2×10^{-3}	1.1×10^{-2}
	Mortality	1.3×10^{-5}	1.1×10^{-5}	1.1×10^{-5}	5.1×10^{-5}
	Morbidity	5.8×10^{-7}	4.9×10^{-7}	4.9×10^{-7}	2.3×10^{-6}
2	Selected		8.9×10^{-2}	8.9×10^{-3}	4.2×10^{-2}
	Mortality		1.1×10^{-4}	1.1×10^{-5}	5.1×10^{-5}
	Morbidity		4.9×10^{-6}	4.9×10^{-7}	2.3×10^{-6}
3	Selected			8.9×10^{-3}	4.2×10^{-2}
	Mortality			1.1×10^{-5}	5.1×10^{-5}
	Morbidity			4.8×10^{-7}	2.3×10^{-6}
4	Selected				2.3×10^{-2}
	Mortality				5.1×10^{-5}
	Morbidity				2.3×10^{-6}

Table 16: Rate of temperature increase of the mixture and IMF, due to disintegration of ^{241}Am is shown in each production area, in each scenario and at each activity level.

Scenario	Activity level	Rate of temperature increase (°C/day) due to ^{241}Am			
		Area 1	Area 2	Area 3	Packaging
1	Selected	2.2×10^{-8}	1.8×10^{-8}	1.8×10^{-8}	8.7×10^{-8}
	Mortality	7.1×10^{-6}	5.9×10^{-6}	5.9×10^{-6}	2.8×10^{-5}
	Morbidity	2.7×10^{-7}	2.3×10^{-7}	2.3×10^{-7}	1.1×10^{-6}
2	Selected		7.3×10^{-7}	7.3×10^{-8}	3.5×10^{-7}
	Mortality		5.9×10^{-5}	5.9×10^{-6}	2.8×10^{-5}
	Morbidity		2.3×10^{-6}	2.3×10^{-7}	1.1×10^{-6}
3	Selected			7.4×10^{-8}	3.5×10^{-7}
	Mortality			5.9×10^{-6}	2.8×10^{-5}
	Morbidity			2.3×10^{-7}	1.1×10^{-6}
4	Selected				1.9×10^{-8}
	Mortality				2.8×10^{-5}
	Morbidity				1.1×10^{-6}

6.7 MDA

Perpetrators may claim to have contaminated IMF using a radioactive source. However, the activity of the source, when and if added, must be enough to be detected in IMF, in order for the contamination to be officially confirmed. This is even if the added activity is far from enough to develop any deterministic effects in infants. Therefore, the minimum amount of added radioactive material that is necessary for enabling detection is investigated. The calculation is based on the MDA of ^{90}Sr, ^{137}Cs and ^{241}Am in a laboratory setting. The investigation continues to a detection system at the facility by introducing two additional activity levels: *MDA level* and *permissible level*. MDA level is the maximum detectable activity concentration in IMF to be detected at a laboratory, as mentioned above. Permissible level is the maximum activity concentration that is allowed in food for trading and consumption. In the calculations, the Derived Intervention Level (DIL) and the Guideline Level (GL) given from the US Food and Drug Administration (FDA) and Codex Alimentarius Commission (CAC), respectively, are used. The detection capabilities at such activity levels from measurements of a single can of IMF are then investigated.

6.7.1 Necessary Activity at Time of Contamination to be Detected at Laboratory

For ^{137}Cs and ^{241}Am sources, the MDA for a High Purity Germanium (HPGe) detector with relative efficiency of 80% is taken from reference [38], as shown in **Table 4**. Even though the reference found the optimal counting time to be between 15 and 20 hours, the MDA given from the counting time of 5 hours is chosen in the calculation. This is to consider the situation being a radiological attack; where the detection and identification of radionuclides must be performed immediately. The MDA is given under the condition where the radionuclides are individually measured using water as a

medium. Thus, the interference from other radionuclides, originally contained in skim milk such as ^{40}K, is not taken into account by the MDA. Therefore, interference due to the preexisting radionuclides is neglected in this work.

For ^{90}Sr source, the MDA for a LS system used to count Cerenkov photons is taken from reference [40]. The MDA of 63.4 Bq/L is given for a counting time of 4 hours under the condition where the radionuclide is dissolved in milk (3% fat content). Assuming that 30 g of IMF dissolved in 200 mL of water, and the density of IMF in readily fed form (in liquid form) is approximated with that of milk [44], the MDA above is equivalent to 470 Bq/kg for IMF in powdered form. The common IMF sold in Norway is in powdered form and has a total fat content of about 3.5 g in 100 mL of readily fed form (in liquid form) [49]. This is equivalent to a fat content of 3.4%. Decrease in count rate due to color quenching is taken into account by the MDA.

The minimum activity necessary, at the time of contamination at the facility, in order for the contamination to be detected from IMF at a laboratory, is shown in **Table 17** for the ^{137}Cs and ^{241}Am sources and in **Table 18** for the ^{90}Sr source in each scenario.

Table 17: Minimum activity of ^{137}Cs and ^{241}Am, at the time of contamination at the facility, to be detected at a laboratory, is shown in each scenario.

Detector type	Radionuclide	Minimum activity necessary at time of contamination (kBq)			
		Scenario 1	Scenario 2	Scenario 3	Scenario 4
P type	^{137}Cs	11.7	2.91	2.90	52.5
	^{241}Am	58.4	14.6	14.5	262

Table 18: Minimum activity of ^{90}Sr, at the time of contamination at the facility, to be detected at a laboratory, is shown in each scenario. A LS system with the counting of Cerenkov photons is assumed to be used.

Radionuclide	Minimum necessary activity at time of contamination (MBq)			
	Scenario 1	Scenario 2	Scenario 3	Scenario 4
$^{90}Sr/^{90}Y$	9.14	2.28	2.27	41.1

6.7.2 Count rate of Sources in a can of IMF at MDA Level at facility

The count rate measured from a can of IMF with the activity at MDA level, using a NaI(Tl) detector in the facility setting, is shown in **Table 19**. The count rates are calculated in the same way as in **Table 8**, **9** and **10**.

Table 19: Count rates measured from a can of IMF with activity at MDA level, using a NaI(Tl) detector in the facility setting, is shown for each radionuclide and in each distance.

Radionuclide	Count rate (cps) in each detection distance (cm)					
	0.5	**2**	**5**	**10**	**25**	**50**
^{90}Sr	2.64	1.74	0.920	0.435	0.0116	3.55×10^{-2}
^{137}Cs	4.18×10^{-2}	2.76×10^{-2}	1.46×10^{-2}	6.89×10^{-3}	1.84×10^{-3}	5.63×10^{-4}
^{241}Am	6.51×10^{-2}	4.30×10^{-2}	2.28×10^{-2}	1.08×10^{-2}	2.86×10^{-3}	8.78×10^{-4}

6.7.3 Count rate of Sources in a can of IMF at Permissible Level at facility

The count rate measured from a can of IMF with the activity at permissible level, using a NaI(Tl) detector in the facility setting, , is shown in **Table 20**. The count rates are calculated in the same way as in **Table 8**, **9** and **10**.

Table 20: Count rates given from a can of IMF with activity at permissible level, using a NaI(Tl) detector in the facility setting, is shown for each radionuclide in each distance.

Type	Radionuclide	Count rate (cps) in each detection distance (cm)					
		0.5	**2**	**5**	**10**	**25**	**50**
FDA	**^{90}Sr**	7.26	4.78	2.53	1.20	0.319	9.76×10^{-2}
	^{137}Cs	6.75×10^{2}	4.45×10^{2}	2.36×10^{2}	1.10×10^{2}	29.7	9.09
	^{241}Am	0.357	0.236	0.125	5.89×10^{-2}	1.57×10^{-2}	4.81×10^{-3}
CAC	**^{90}Sr**	4.30	2.84	1.50	0.710	0.189	5.80×10^{-2}
	^{137}Cs	5.34×10^{2}	3.52×10^{2}	1.86×10^{2}	88.1	23.5	7.19
	^{241}Am	0.167	0.114	5.84×10^{-2}	2.76×10^{-2}	7.35×10^{-3}	2.25×10^{-3}

6.8 Chemical Procedures for ^{90}Sr and ^{241}Am Sources

The ^{90}Sr source from a Radioisotope Thermoelectric Generator (RTG) and the ^{241}Am source from smoke detectors, selected in this work, are insoluble to water. In order for these sources to be effective, when used in an attack targeting IMF, the sources are preferred to be soluble to water to be evenly distributed in the IMF. One approach is to obtain the radionuclides as water-soluble compounds in a powder form. However, this approach is time consuming, since it requires using a series of chemical procedures. The longer time is spent for the procedures, the higher amount of absorbed dose would be received by the perpetrators. Therefore, perpetrators may, instead, dissolve the sources in an acid mixture and obtain water-soluble compounds of the radionuclides in a liquid form. Another approach is to grind the sources into a powder. However, it may sink to the bottom of the tank, instead of being evenly distributed and transferred to the final product, i.e. a can of IMF. This results in the attack being unsuccessful.

Adding a solution into a tank may also bring some difficulties such as:

1) The added volume of the solution that is transferred to the tank;
2) The shielding necessary for such a volume to avoid developing deterministic effects to perpetrators during transportation;
3) The change in pH inside the tank (if quality checks are routinely performed at the facility by checking the value of pH); and
4) The precipitation caused in the tank due to the change in pH when dilution happens.

The consequences of 1) and 2) can be minimized simply by dissolving the sources in a strongly corrosive acid. However, this may maximize the consequences of 3) and 4). Therefore, at least reduction of acidity should be performed after dissolving the sources to the acid. The procedures introduced below are only suggestions based on literature research, not on actual laboratory works. Therefore, the certainty of the methods and the yields of the compounds obtained are not investigated in this work.

6.8.1 Dissolution of ^{90}Sr Sources

The ^{90}Sr source, originally in the form of $^{90}SrTiO_3$ and age of 37 years, approximately contain ^{90}Sr : ^{90}Zr in a 1.2 : 1.7 molar ratio. ^{90}Zr is a stable nuclide and generated due to the disintegration of ^{90}Y. The number of ^{90}Y atoms is 8 orders of magnitude less than that of ^{90}Sr and ^{90}Zr atoms, and therefore neglected. Dissolution of $SrTiO_3$ is successfully demonstrated in a reference [59] using the acid mixture of HNO_3 : H_2O_2 : HF = 16 : 2 : 1 in molar ratio. When the ^{90}Sr source is dissolved, ^{90}Sr is assumed to form either tetravalent complex $^{90}SrF_6^{2-}$ or $^{90}SrF_2$ [60]. $^{90}SrF_2$ is soluble in concentrated HNO_3 solution [61]. Ti is assumed to form either a tetravalent complex, such as TiO_2^{2+}[62] with H_2O_2 [63], or another tetravalent complex TiF_6^{2-} with HF [64]. ^{90}Zr is assumed to dissolve in the mixture and form Zr^{4+} [41]. After dissolving the source, Ti precipitates as TiO_2 [64] by increasing the pH of the solution to 3 [60]. Over 90% of Zr precipitates as $Zr(OH)_4$ at pH 3.5[41]. Thus, this method gives a solution of ^{90}Sr at pH of 3.5 without majority of Ti and Zr that would otherwise precipitate in a tank.

6.8.2 Dissolution of ^{241}Am Sources

The ^{241}Am source, as described in **Section 5**, contain ^{241}Am, Au and Ag. The number of Au and Ag atoms is 4 and 5 orders of magnitude, respectively, greater than that of ^{241}Am atoms. Au dissolves in the acid mixture of HCl : HNO_3 in a 3 : 1 molar ratio, and forms a chloro-complex of $[AuCl_4]^-$. AmO_2 is assumed to also dissolve in the acid mixture. This is based on the fact that AmO_2 dissolves in the excess amount of 6 M HCl solution when heated [61]. When dissolved, AmO_2 is assumed to form Am^{3+}. On the other hand, Ag forms a layer of insoluble AgCl onto its surface. Some amount of AgCl dissolves in a high concentration of HCl solution and forms chloro-complexes of $AgCl_n^{1-n}$, such as $AgCl_2^-$ and $AgCl_3^{2-}$. After dissolving the source, Au precipitates as AuO(OH) by increasing the pH of the solution [65]. Majority of $AgCl_n^{1-n}$ precipitates as AgCl when pH of the solution increases. Thus, this method gives a solution of ^{241}Am without majority of Au and Ag that would otherwise precipitate in a tank.

7 Discussion

7.1 Effectiveness of Contamination Scenario

The most effective contamination scenarios, in terms of dilution rate of activity from the time of contamination to a single can, are **Scenario 2** and **3** with a factor of 4 greater than that of **Scenario 1**, as seen in **Table 27**. However, **Scenario 1** has the ability to contaminate 24 125 cans at once, while **Scenario 2** and **3** "only" contaminates 6 031 cans, which is the factor of 4 less. **Scenario 4**, the only one that perpetrators may conduct from the outside of the facility without physically entering, is the least effective. This is because the majority of activity at the time of contamination escapes with the outlet air during the spray drying.

7.2 Deterministic Effects to Infant Caused by Selected Activity Level

When an infant ingests a *single* serving (24.6 g) of IMF contaminated with ^{90}Sr and ^{137}Cs with the activity at selected level, the absorbed dose to its large intestine and bone marrow will easily exceed the threshold of the gastrointestinal syndrome and hematopoietic syndrome. This is regardless of which of the contamination scenarios are chosen, as shown in **Table 29**. With such an absorbed dose, all infants who have ingested a single serving of contaminated IMF will most likely have effects that result in mortality.

On the other hand, the absorbed dose received from a *single* serving of IMF, contaminated with ^{241}Am with the activity at selected level, stays far below the threshold of the hematopoietic syndrome. The absorbed dose to abdomen of an infant, received from *consecutive* feedings of the IMF, finally reaches the threshold of prodromal syndromes on day 4 for **Scenario 1** and day 2 for **Scenario 2** and **3**. In this case, the infants who have ingested the radionuclide may be in position to receive prompt and correct radionuclear decorporation to avoid developing the hematopoietic syndrome. The total absorbed dose received from the consecutive servings mentioned above seems to reach threshold of hematopoietic syndrome within several months after the ingestion in all scenarios, as shown in **Figure 5**. This is due to a *daily* absorbed dose given to a specific organ (the bone marrow in this case) by some radionuclides, such as ^{90}Sr and ^{241}Am, being relatively nearly completely retained long after ingestion, as shown in **Figure 13**. This is largely influenced by the organ's affinity of the radionuclides.

Deterministic effects such as the hematopoietic syndrome occur when a large number of cells are killed due to radiation. However, the degree of the cell killing is influenced by the repairing rate of sub-lethal damage within cells that are exposed to radiation. Additionally, undamaged cells repopulate within a few days to weeks after the exposure [33]. Therefore, the hematopoietic syndrome may not occur, even when the total absorbed dose reaches the threshold of the syndrome several months after the ingestion. However, it must be noted that the given thresholds of the gastrointestinal and hematopoietic syndromes are based on the symptoms of the syndromes to occur with 1% of risk to an adult, not to an infant. Therefore, the thresholds for the syndromes to an

infant may be lower than this work accounts for, due to the rapid growing and developing status of infant.

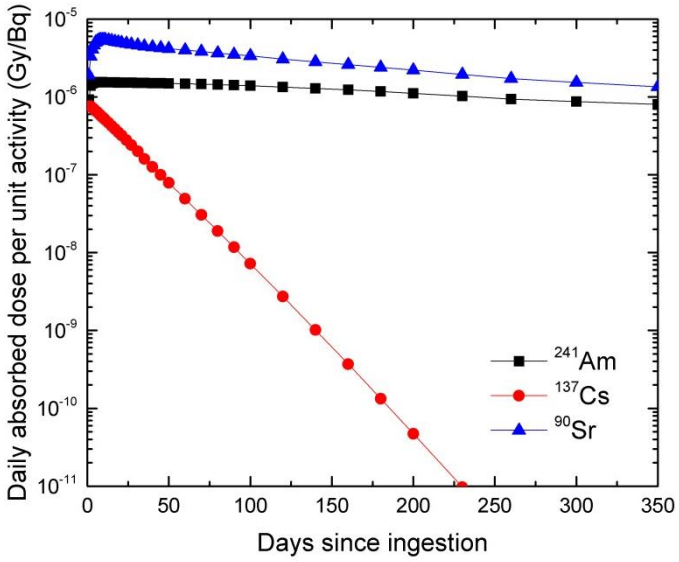

Figure 13: *Daily* absorbed dose per unit activity to the bone marrow of an infant, received from a single ingestion of each radionuclide on day 1, is shown [29].

The difference in the absorbed doses given to the infant, from the three sources, is mainly due to the amount of activity selected for each source: the activity at selected level for ^{90}Sr and ^{137}Cs is approximately the 6 and 5 orders of magnitude greater than that of ^{241}Am, respectively. When the radionuclides with the equal disintegration rate are ingested by the infant, the highest total absorbed dose to the bone marrow, from a single ingestion on day 1, is given from ^{90}Sr, as shown in **Figure 14**. The difference in the doses from ^{90}Sr and the other two, however, is a factor of 7 on day 10, not several orders of magnitude.

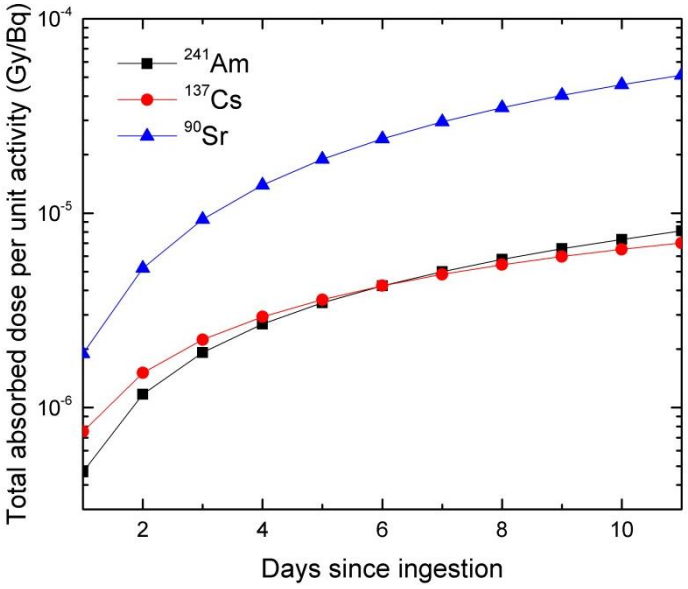

Figure 14: Total absorbed dose per unit activity to the bone marrow of an infant, received from a single ingestion of each radionuclide on day 1, is shown.

7.3 Count Rate Measured from a Can of Contaminated IMF

The count rate due to indoor background radiation measured using a NaI(Tl) detector, with a normal and practical amounts of shielding around it, is assumed as 5 cps. Therefore, it would be appropriate for the detector system to trigger an alarm for abnormal radioactivity, if the total count rate detected exceeds 15 cps, i.e. three times the background count rate of the background radiation. Assuming that a can of IMF is in a fixed position and not moving, all of the activity levels of the contamination with ^{137}Cs sources will easily give count rates that are above 15 cps, i.e. the alarm level, in any of the detection distance calculated. For the contamination with ^{90}Sr and ^{241}Am source, a majority of activities investigated in this work give count rates that are above 15 cps in any of the detection distance calculated. The only cases in which abnormal radioactivity would not be seen is the activity at morbidity level (when the detection distance is 50 cm) for the ^{90}Sr source. For the ^{241}Am source, the activity at selected level in **Scenario 3** (when the detection distance is 25 cm and 50 cm) and **Scenario 4** (when the detection distance is 10cm, 25cm and 50 cm) would not be seen as abnormal radioactivity. Therefore, as long as the detector is placed fairly close to a can, abnormal radioactivity that can potentially cause deterministic health effects to an infant by ingestion can be detected, before the cans are widely distributed. However, if the cans are in a mobile position, such as when placed on a moving belt conveyer, the count rate measured by the detector from the cans would be decreased. This is due to the constant change in the detection distance, as well as the short counting time for each can. Therefore, in such a case, the smallest possible detection distance should be chosen in order to detect abnormal radioactivity. The rate of decrease in count rate due to the mobile position is not investigated in this work. However, if a manufacturing facility has an ability to adopt a minor modification in its production line during packaging, the efficiency of detecting abnormal radioactivity would be largely improved. For example, by positioning the detector system as shown in **Figure 15** [66].

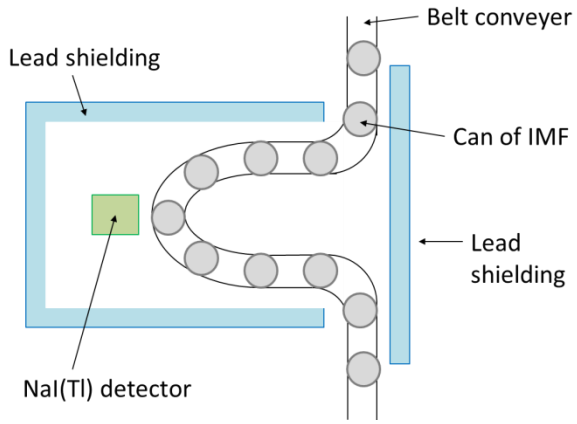

Figure 15: Schematics of the positioning of a NaI(Tl) detector system at a package site of the facility from above. The path of a belt conveyer is looped in order to create a detection area. The area is surrounded by lead shielding. Another lead shielding is placed on the other side of the belt conveyer. Lead shielding is also placed above and below the detection area.

Lead shielding is placed in such way that the background radiation, occurring outside the detection area and emitted toward the detector, is absorbed by the shielding. Therefore, the detector receives

minimum of background radiation signals. Thus, the alarm level, 15 cps, would largely be decreased. The degree of the background radiation decreased in this way is not investigated in this work.

In order to obtain even more realistic calculations, a computer simulation program (such as Monte Carlo) can model the detection rate and sensitivity by, in detail, calculating the behavior of a large number of γ rays (or other types of radiation) in well described system based on the well-known physical absorption processes of electromagnetic radiation (and other types of radiation). There is available special tool-kits for such calculations that are widely used in the scientific community, e.g. the GEANT4 tool-kit from the European Organization for Nuclear Research (CERN) [67-69]. For the assessment of the count rate of the γ rays, the simulation can overcome several approximations and assumptions in the calculation such as; the point source; the interaction distance of the γ rays with the IMF and the tin; and the count rate of scattered γ rays. In this work, the interaction distance was assumed to be a minimum, as if all of the γ rays counted are emitted perpendicularly to the detector. For the assessment of the count rate of the β particles, the simulation can especially overcome the critical assumption in the calculation. That is, the energy of the β particles to be a single value, not a continuous spectrum. Therefore, a simulation can improve the calculation further (in addition to the case of the γ rays) by correctly assessing the energy of the β particles lost due to the attenuation with the IMF, tin and air. This is achieved by applying a proper value of stopping power that corresponds to the energy of each β particle. Therefore, the simulation also improve the correct assessment of the fraction of the β particles that pass through the tin layer and reach the detector with sufficient amount of energy to generate signals, i.e. count rate. In order to improve the calculation in the case of ^{90}Sr source, the count rate of the β particles emitted from ^{90}Sr should also be added to that of ^{90}Y.

There are more than a dozen radionuclides that are pure β emitters, in addition to ^{90}Sr/^{90}Y, and their β particle energies are relatively low compared to that of ^{90}Y. In such cases, bremsstrahlung generated from IMF and the material of the can may be used in order to detect abnormal radioactivity. Using a Monte Carlo simulation may be particularly useful in calculating such a count rate. This is partially due to the thickness of the material of a can. Some β particles lose their total energy that is left when they reach the material layer to the material. In this case, the fraction of the energy converted to bremsstrahlung photons can be calculated using corresponding radiation yield to the energy of β particles when reaching the material. However, some β particles lose only a part of energy that is left when they reach the material layer to the material. In this case, the corresponding radiation yield cannot be used to calculate the fraction of the energy converted to bremsstrahlung photons. Therefore, the calculation becomes complicated, and thus the use of a Monte Carlo simulation may be essential to achieve a realistic assessment of the count rate of the bremsstrahlung photons. In this work, the investigation is limited to the selected radioactive sources due to the time restraints of the project.

7.4 Deterministic Effects to Workers

For deterministic effects caused by external exposure to γ rays and bremsstrahlung photons, the symptoms of the prodromal syndrome caused by external exposure, such as anorexia, nausea, fatigue, vomiting and diarrhea, are of interest. The thresholds of these symptoms range between 1.0 Gy and 2.3 Gy, and is based on the occurrence of each symptom in 50% of adults.

For the contamination with ^{90}Sr and ^{241}Am sources, the absorbed dose rate given from any points of production, in any scenarios, and at any activity levels, is far from enough to cause any symptoms of

prodromal syndrome in workers. Regarding contamination with the ^{137}Cs source, the potential places in the production facility where symptoms of prodromal syndrome in workers may be developed are the storage/mixing tank in **Area 1** in **Scenario 1**, that in **Area 2** in **Scenario 2**, that and in **Area 3** in **Scenario 2** and **3**, all with the activity at selected level. Among those, the highest absorbed dose rate given is the tank in **Area 2** with 0.83 Gy/h. The mixture in the tank in **Area 1** is distributed to four of the tanks in **Area 2** with each of them operating 10 batches. In **Scenario 2**, the contamination occurs only to one of the four tanks in **Area 2** with only one out of 10 batches. Assuming that the process of mixing takes 2 hours per batch, a worker receives 1.65 Gy. This assumes that the same worker is placed by the tank with a contaminated mixture for a period of 2 hours[2]. This absorbed dose may potentially cause anorexia, nausea and fatigue to the worker, while he/she is on duty. The worker must be in position (50 cm away from the tank) for a total of at least 1.2 hours and 1.8 hours, in order to develop anorexia and fatigue, respectively. However, development of these symptoms in only one worker may be easily confused with other common illnesses. Thus, it may not be seen as an ongoing abnormality in the production. In the case of the storage tanks in **Area 1** and **3**, the absorbed dose rates given are 0.17 Gy/h and 0.30 Gy/h, respectively. Those are storage tanks, and in this case the contaminated mixture may be kept for days, not hours. A total of at least 5.9 hours and 3.3 hours are necessary for the tanks in **Area 1** and **3**, respectively, to result in developing anorexia in a worker. However, since it is a storage tank, it is not likely that the worker is placed in the position for such a long period. Hence, with all of the sources, in any scenario and at any activity level investigated in this work, it is assumed that development of deterministic effects in workers will not alarm ongoing abnormality in a production.

In order to obtain even more realistic calculations, a Monte Carlo simulation can also be applied for assessment of the absorbed dose rate given from the γ rays and the bremsstrahlung photons. In the case of the bremsstrahlung photons, the simulation overcomes another critical assumption in the calculation. That is, the energy of the bremsstrahlung photons being a single value, not a continuous spectrum. The simulation may further improve the calculation such as the angular dependency of bremsstrahlung photons, in addition to what has been mentioned earlier. In order to improve the calculation in the case of ^{90}Sr source, the bremsstrahlung photons generated by the β particles emitted from ^{90}Sr should also be added to that of ^{90}Y. In this work, this simulation is not performed due to the time constraint of the project.

7.5 Rate of Temperature Increase

The rationale of the investigation on the rate of temperature increase in mixture and IMF is to seek out a potential method that makes it possible to detect abnormal radioactivity, using different physical properties of the radionuclides than the radioactivity. However, the calculated rate for all of the sources, in any of the scenarios and at any activity level, seems to be far from enough to be detectable.

Regarding contamination with the ^{90}Sr source with activity at selected level, the mixing tank in **Area 2** in **scenario 2** gives the rate of 0.97 °C/day. However, the mixing process is assumed to be for 2 hours,

[2] How realistic it is that a worker will be positioned close to a production tank for 2 hours is of course open for discussion. Today, most processes are automated and the workers rarely spend extended periods of time close to the tanks. However, for this work, a sort of worst-case scenario where a worker spends prolonged periods of time close to the tank is imagined.

and therefore the actual temperature increase obtained from the tank is 0.081 °C. Thus, the highest possibility to detect the increase in temperature would be given by the can in packaging in **Scenario 3** with 0.46 °C/day. Yet, a detection device, such as a thermal camera, often has the uncertainty of about ±2% [70]. Assuming that the room temperature inside the facility is 15 °C, the temperature increase of 0.3 °C from the can, compared to its surroundings, is required at all times in order to detect an abnormality. The heat generated from ^{90}Sr source inside the can will constantly be lost, through the material of the can, to its surroundings. Therefore, the balance between generation and loss of heat will be established after equilibrium. This results in the can to be constantly at a higher temperature than a normal can. However, the temperature increase of 0.3 °C (65% of generated heat a day in this case) may not be difficult to achieve.

7.6 MDA

Comparison of **Table 17** and **18** with **Table 32** shows that the activity at MDA level, in a laboratory setting using a HPGe detector and a LSC, is about2, 6 and 5 orders of magnitude lower than that of the morbidity level for ^{90}Sr, ^{137}Cs and ^{241}Am, respectively.

For ^{137}Cs and ^{241}Am, the MDA used in the calculation (counting time of 5 hours) is a factor of 2 greater than that given from the optimal counting time (15-20 hours), as found in the reference [38], for both of the radionuclides. However, these MDAs are still several orders of magnitude below the permissible level for what is the legal limit of radionuclide content in food, as shown in **Table 5**. Since the interference from other radionuclides that naturally exist in skim milk is not considered in the given MDAs, the minimum activity necessary at the time of contamination may, in reality, become slightly greater than that obtained in the calculation. In the case of ^{241}Am, the MDA given from a longer counting time may be applied, if the interference from other preexisting radionuclides is significant.

For ^{90}Sr, milk is used to dissolve the source in the reference [40] for the given MDA. The fat content of IMF is 0.4% lower than the milk. Therefore, the necessary activity may also be expected to be slightly greater than what was obtained in the calculation. However, the given MDA is still at about a factor of 2.7 and 1.6 below the permissible level for FDA and CAC, respectively.

Minimum count rate, in order to detect abnormal radioactivity at the facility, can largely be affected by the count rate of background radiation as well as the counting time of a can. The count rate of background radiation can be minimized as shown in **Figure 15** and in many other similar ways by building effective shielding or more advanced detector systems. Therefore, the main difficulty of detecting small amount of activity at the facility remains in the counting time. However, the counting time must be sufficiently short (ideally set to a few seconds up to a minute) in order not to affect the production. This is especially important if the can is not in a still position, for example when on a moving belt conveyer. This could be significantly improved, for example, by counting several cans (that are randomly selected) at once for a much longer time, instead of counting every can. This, however, would not detect instances where only a single can has been contaminated.

The detection at the facility is performed by measuring from the outside of the can. Therefore, the γ rays and the β particles emitted from the sources inside of the can must penetrate IMF and the can walls in order to reach the detector. The interaction with the tin layer is calculated to decrease the intensity of the γ rays from ^{241}Am significantly to 38.3%, while that from ^{137}Cs remains 98.8%. In the

case of β particles from ^{90}Y, the β particles reaching the detector, after interacting with the IMF and the tin layer, are calculated to be only 6.4% (with uncertainty of ±3.8%) of the β particles originating inside the can. If the facility has a possibility to use aluminum as the material of a can, the intensity of γ rays from ^{241}Am is calculated to remain 98.5%. The ratio of β particles reaching the detector increases to 30.7% (with uncertainty of ±18.6%)

In the case of the MDA level, the count rates given from the activities are far from enough to alarm about an abnormal radioactivity in the facility for all of the sources. In the case of the permissible level, the activity of ^{137}Cs easily alarms an abnormality in any detection distance investigated, while that of ^{241}Am is far from enough to alarm. The activity of ^{90}Sr may alarm an abnormality if the detection distance is sufficiently short. However, since the uncertainties in the calculation are large, this will vary.

7.7 Chemical Procedures for ^{90}Sr and ^{241}Am Sources

Radiation protection is necessary for the perpetrators, throughout the chemical procedures as well as during the transportation of the solution, until an attack has been carried out. This is because even if they are ready to sacrifice their own lives, developing severe deterministic effects can prevent them in the process. In order to avoid receiving excess amount of absorbed dose, a perpetrator may consider minimizing the amount of the sources dissolved at a time. However, dividing the dissolution procedure into several batches becomes time consuming and the perpetrator receives an absorbed dose during the procedure. An absorbed dose received from each batch will still be summed up, even though a decrease in absorbed dose rate would help recovering damaged DNA each time. Therefore, this approach gives no gain to the perpetrator. The best approach would be to use shielding with suitable material and thickness. The shielding is also necessary during the transportation of the solution. This will complicate the transportation process, since adequate shielding can be quite heavy and large.

In the case of ^{90}Sr source, external exposure due to β particles emitted from ^{90}Sr and ^{90}Y, as well as bremsstrahlung photons generated by the β particles in a solution and surrounding materials are to be considered. In order to completely shield the maximum energy of the β particles from ^{90}Y, i.e. the highest energy of all in this source, a plastic shielding with the thickness of 1.3 cm is necessary. In order to shield the majority of bremsstrahlung photons, that mainly distributed in a range between 50 keV and 400 keV [57, 58], a lead shielding with the maximum thickness of 2 cm is necessary. The lead shielding must be placed between a perpetrator and the plastic shielding. This is to avoid further generation of bremsstrahlung photons in the lead shielding, since much more bremsstrahlung photons are generated in material with high atomic number than that with low atomic number.

In the case of the ^{241}Am source, external exposure due to γ rays emitted from ^{241}Am is to be considered. In order to completely shield the γ rays with the energy of 60 keV, a lead shielding with the thickness of 0.1 cm is necessary.

In addition to the shielding, a mirror can be placed above the working area while dissolving the sources. This makes possible to operate and complete the procedures behind the shielding, which results in protection for the eyes and head area from external exposure. This is especially needed if the source contains very high activity. With such an activity, protecting hands and arms from external exposure is also necessary. Clamps, thongs and other remote manipulation tools may be used in

order to complete all of the procedures behind the shielding, while minimizing exposure to the hands.

Regarding the difficulties in adding the solution into a tank, as mentioned in **Section 6.8**, the degree of the consequence given from the precipitation caused in the tank due to the change in pH, when dilution happens, may depend on factors such as; the amount of precipitation; the flow rate of the mixture poured into the solution; and the mass ratio of total solids content to the mixture in the tank. The effectiveness of the contamination will largely be affected if the precipitations contain ^{90}Sr and ^{241}Am. This is because they may sink to the bottom of the tank, instead of being evenly distributed and transferred to the final product (a can of IMF). In the case of ^{137}Cs source, $^{137}CsCl$ is water soluble, and therefore it is expected to give its maximum effectiveness to the contamination in its original form. With the dissolution methods mentioned earlier in this work, ^{90}Sr and ^{241}Am are assumed to form water-soluble $^{90}Sr(NO_3)_2$ and $^{241}AmCl_3$. Therefore, the concern regarding the effectiveness of contamination can be neglected. Thus, the only concern left is the precipitation formed by other nuclides. If they sink to the bottom of the tank, it may alarm an ongoing abnormality in the production. On the other hand, if they are dispersed evenly in the mixture, the contamination is not noticeable. The mixture contains stabilizers and emulsifiers, and these may contribute to keep the precipitations in the mixture and form colloids. If that is the case, the same effect would be applicable to sources that are made into a powdered form, for example using a grinder, without any chemical procedures. This is if the size of the particles that are ground is sufficiently small. In this work, chemical effects given from the addition of stabilizers and emulsifiers to the sources of contamination are not investigated.

7.8 Potential of Radiological Attack Compared with Other CBRN Attacks, Traditional Attacks and the September 11th Attack

Nuclear weapons require state of the art technology, in addition to actually obtain (or produce) plutonium or highly enriched uranium. They would be the most challenging of any CBRN attack. Chemical, biological and radiological agents, in readily usable form and in a large quantity, are not easily accessible either. Therefore, such programs, in the cases of chemical and biological agents, have historically been conducted with governmental involvement [71, 72]. However, since the collapse of the former Soviet Union in 1991, large black markets of *refined* CBRN agents have been thriving under the radar [73]. In addition to this, the recent civil war in Syria (that started in 2011 and still continuing to date) may have become the latest contribution to this black market [74], making refined CBRN agents even more accessible.

On the contrary to refined CBRN agents, there are *crude*-type of chemical, biological and radiological agents, which is one of the focus points in this work. Necessary agents in crude form are stored at civilian facilities (educational/research institutions, commercial industries or medical hospitals and facilities). Some agents are available to anyone as commercial products in regular stores, such as smoke detectors equipped with ^{241}Am. Even though the amount of agents contained in a single product may be extremely small, collecting tens of thousands of these products would pose a possible threat. The crude-type CBRN attack is logistically more advanced than that of a conventional attack, which requires the lowest amount of technology if any, techniques and tools, such as use of a

truck or a knife against soft targets. However, the crude-type CBRN attack can cause a much greater physical, psychological and economic impact, if successfully carried out.

Limiting the case to an attack to contaminate IMF, as described in this work, the effectiveness of chemical, biological and radiological attacks, regardless to the use of refined or crude-type of agents, would be mainly determined by factors such as: physicochemical form of the agent at the time of contamination; and durability of the agent to heat and wetness. In terms of physicochemical form, using the agent in a gas form at the time of contamination, except in **Scenario 4**, would be much harder than that in a liquid or solid form. In the case of liquid form, miscibility to water may not play an important role due to addition of emulsifiers and stabilizers to IMF mixtures during the production. In the case of solid form, the agent should be finely ground for the best possible effectiveness, if insoluble to water (or rather milk). In terms of the durability to heat, biological agents would not survive through the spray drying process at 180 °C. The temperature used to sterilize biological agents, such as Anthrax and Plague, is 121 °C [75, 76]. In terms of the durability to wetness, many chemical agents hydrolyze [77] and result in different chemical compounds that may not be as toxic as initially expected for the agents, even though they would still be toxic. However, it must be noted that some chemical agents, such as a vomit agent Adamsite, form toxic oxides by hydrolysis [77]. The degree of occurrence in hydrolysis of the agents, within the temperature range used in the facility, is individual to each agent. This is because the degree depends on each reaction being exothermal or endothermal. In the case of radiological agents such as ^{90}Sr, ^{137}Cs and ^{241}Am, their compounds mentioned in this work ($^{90}Sr(NO_3)_2$, $^{90}SrTiO_3$, $^{137}CsCl$, $^{241}AmO_2$ and $^{241}AmCl_3$) are stable to heat within the range used in the facility. Hydrolysis of the compounds, even if any, would not affect their toxicity since radiological toxicity originates in each radionuclide, not its compound. Based on these facts, the radiological agents would give the highest ability in achieving the effect that is initially expected for the agent, in the case of contamination of IMF. In the case of contaminating other processed foods, each type of agents may demonstrate different ability from what is discussed above. This is because the type of processed food determines the range of temperature and pH used, the manufacturing process, such as from wetness/dryness to production line being sealed/unsealed.

The effectiveness of the contamination, in terms of spreading negative health effects to general public, can be brought by difference in the nature of chemical, biological and radiological agents. That is, ability to infect others. Some biological agents, such as Plague, are extremely infectious [78]. A person who has been infected by an infectious biological agent will further infect others and spread the same type of negative health effect. If the biological agent is one of those that health authorities expect to diagnose occasionally, it may cause a delay in discovery of the outbreak. A person who has ingested a chemical or radiological agent will not give the same type of negative health effects to others. In the case of radiological agent, the person will, instead, give some amount of absorbed dose to others from external exposure due to γ rays and bremsstrahlung photons emitted from the body of the person. However, the effect from this would be extremely small. If the person develops distinct symptoms that are unique to health effects caused by radiation or chemicals, a large investigation would immediately take place.

In the case of a crude-type attack, the agents used for a contamination must be prepared before carrying out the attack. One of the difficulties of the crude-type attack may also come down to the nature of the agents, as mentioned above, during the preparation process: That is, spreading negative health effects to others, including all perpetrators, if more than one. If civilians are infected

during the preparation, a large investigation could take place before the actual attack is even carried out. Further difficulties of the crude-type attack, during the preparation process, may lay on another nature of the agents: That is, physicochemical form of the agent during the preparation process. In the case of the radiological agent, the origin of hazard is clear as long as the agent is dissolved in a solution, as mentioned in **Section 7.7**. The chemical and biological agent, however, may escape in air, which would make it harder to avoid, unless a proper ventilation system is equipped in the work area.

Lastly, as mentioned in **Section 2**, some perpetrators may have an ambition to obtain media attention (similar to that of the September 11th attacks in the US). It is scientifically difficult to compare the impact of the September 11th attacks with the attacks investigated in this work. However, in terms of fatality, the September 11th attacks resulted in 2977 fatalities in total where 2753 of those occurred in the World Trade Centers [26]. To emphasize the importance and discoveries made in this work, the radiological attack described in **Scenario 1** produces 24 125 cans of contaminated IMF and that in **Scenario 2**, **3** and **4** produces 6 031 cans. These cans will, of course, not be delivered to retailers at the exact same time. Some retailers may have a certain numbers of cans from previous deliveries left in store. Due to these, the contaminated cans will not be purchased at the exact same time. Assuming that 10% of the cans are being used before the attack is discovered. Depending on the amount of activity added, fatality from this radiological attack may be comparable to that of the September 11 attacks.

8 Conclusion

Based on the assumption that the deliberate radiological attack investigated in this work is successful, there is a potential of a considerably large number of infants that would receive negative health effects, i.e. mortality or morbidity, due to the ingestion of radionuclides in contaminated IMF. This largely contradicts the conclusion made by the majority of literature that in the scenarios described mainly focus on methods such as RDD. That is, even when a radiological attack is successfully carried out, it is expected to cause a very small number of casualties. However, the radioactivity released from contaminated IMF at the mortality and morbidity levels are detectable, during the production, if the facility is capable of placing a NaI(Tl) detector or other appropriate detectors at the packaging site. The detection can be performed from the outside of its packaging (a can), and therefore the production line would not be negatively affected. In the case of contamination at permissible level, the detector would successfully alarm the abnormality only for the ^{137}Cs source. Yet, permissible level of contamination causes no negative health effects even if the radionuclides are ingested. In order to prevent public fear and panic, clear and sensible communication is highly recommended between the responsible organizations and the general public.

This investigation has also discovered another important fact. That is, the radioactive sources that are easily accessible to the general public (such as those in domestic smoke detectors) make for the possibility of a crude-type attack. In the case of the ^{90}Sr and ^{241}Am sources selected in this work, the original physicochemical forms of the sources make the attack difficult, but not impossible if the perpetrators are fully committed. Improving the physicochemical forms of easily accessible radioactive sources may be an approach to prevent the crude-type attack. However, more importantly, another approach such as to place a NaI(Tl) detector in food industries would be much needed.

Lastly, even though the scope of this work, in terms of consequences, is limited to scientific facts, i.e. negative health effects to individuals, it would be very possible that the type of radiological attack described in this work would bring further consequences such as: an economic impact on the brand and the industry due to the fact that IMF is targeted; an economic impact on the facility due to decontamination of its production line; and loss of public confidence.

References

[1] The US Food and Drug Adnimistration, CARVER + Shock Primer: An Overview of the CARVER Plus Shock Method for Food Sector Vulnerability Assessment. <https://www.fda.gov/food/fooddefense/fooddefenseprograms/ucm376791.htm>, 2009 (accessed 5.4.2017).
[2] E. Croddy, C. Perez-Armendariz, J. Hart, Chemical and biological warfare : a comprehensive survey for the concerned citizen, Copernicus Books, New York, 2002.
[3] A.A. Fries, C.J. West, Chemical warfare, New York etc.: McGraw-Hill Book Company, inc., 1921.
[4] Crisis Management and Fight Against Terrorism, Directorate A "Internal Security", Directorate-General Home Affairs, European Comission, CBRN Glossary. <https://ec.europa.eu/home-affairs/sites/homeaffairs/files/what-we-do/policies/crisis-and-terrorism/securing-dangerous-material/docs/cbrn_glossary_en.pdf>, (accessed 1.5.2017).
[5] C. Wirz, E. Egger, Use of nuclear and radiological weapons by terrorists?, International review of the Red Cross 87(859) (2005) 497-510.
[6] K. Ivanova, T. Sandler, CBRN Attack Perpetrators: An Empirical Study, Foreign Policy Analysis 3(4) (2007) 273-294.
[7] S. Cavallini, F. Bisogni, M. Mastroianni, Economic Impact Profiling of CBRN Events: Focusing on Biological Incidents, Archivum Immunologiae et Therapiae Experimentalis 62(6) (2014) 437-444.
[8] K. Ivanova, T. Sandler, CBRN Incidents: Political Regimes, Perpetrators, and Targets, Terrorism and Political Violence 18(3) (2006) 423-448.
[9] D.C. National Defense Univ Washington, Chemical, Biological, Radiological, and Nuclear Terrorism: The Threat According to the Current Unclassified Literature, 2002.
[10] C.D. Ferguson, M.M. Smith, Assessing Radiological Weapons: Attack Methods and Estimated Effects, Defence against Terrorism Review 2(2) (2009) 16.
[11] K.G. Andersson, T. Mikkelsen, P. Astrup, S. Thykier-Nielsen, L.H. Jacobsen, S.C. Hoe, S.P. Nielsen, Requirements for estimation of doses from contaminants dispersed by a 'dirty bomb' explosion in an urban area, J. Environ. Radioact. 100(12) (2009) 1005-11.
[12] International Atomic Energy Agency, The Radiological Accident in Goiânia, Vienna, 1988.
[13] R.P. Gale, Lax Eric, Radiation: What it is, what you need to know, Knopf2013.
[14] K.G. Andersson, T. Mikkelsen, P. Astrup, S. Thykier-Nielsen, L.H. Jacobsen, L. Schou-Jensen, S.C. Hoe, S.P. Nielsen, Estimation of health hazards resulting from a radiological terrorist attack in a city, Radiat. Prot. Dosim. 131(3) (2008) 297-307.
[15] International Atomic Energy Agency, The Radiological Accident in Lia, Georgia, Vienna, 2014.
[16] C.D. Ferguson, T. Kazi, J. Bīrīrā, Commercial radioactive sources: surveying the security risks, Monterey Institute of International Studies, Center for Nonproliferation Studies Monterey2003.
[17] Utenriksdepartementet Oslo (Norway), The Norwegian Plan of Action for nuclear safety issues (NEI-NO--892), 1997.
[18] S. Coll, THE UNTHINKABLE: Can the United States be made safe from nuclear terrorism?, The New Yorker, US, 12.3.2007.
[19] T. McTague, Did torture stop UK terror attack? Al-Qaeda terrorist captured in London after CIA spies interrogated Guantanamo Bay detainee, Daily Mail, UK, 12.12.2014.
[20] M. Schreuer, A.J. Rubin, Video found in Belgium of nuclear official may point to bigger plot, The New York Times, US, 18.2.2016.
[21] International Atomic Energy Agency, IAEA Incident and Trafficking Database (ITDB): Incidents of nuclear and other radioactive material out of regulatory control. 2016 Fact Sheet. <https://www-ns.iaea.org/downloads/security/itdb-fact-sheet.pdf>, 2016 (accessed 12.4.2017).
[22] C. Mortimer, Nato warns there is 'justified concern' Isis will carry out nuclear attack in Europe, Independent, UK, 19.4.2016.

[23] International Atomic Energy Agency, Methods for Assessing Occupational Radiation Doses Due to Intakes of Radionuclides, Vienna, 2004.
[24] A. Tofani, M. Bartolozzi, Ranking Nuclear and Radiological Terrorism Scenarios: The Italian Case, Risk Analysis 28(5) (2008) 1431-1444.
[25] C.D.K. Ferguson, T.; Perera, J., Commercial radioactive sources, Center for Nonproliferation Studies, Monterey Institute of International Studies, Monterey, CA, 2003.
[26] CNN Library, September 11, 2001: Background and timeline of the attacks, CNN, 8.9.2016.
[27] F.H. Attix, Introduction to radiological physics and radiation dosimetry, John Wiley & Sons2008.
[28] J. Valentin, The 2007 recommendations of the international commission on radiological protection, Elsevier Oxford, UK2007.
[29] US Environmental Protection Agency, Radiation Protection: DCAL Software and Resources. <https://www.epa.gov/radiation/dcal-software-and-resources>, (accessed 3.4.2017).
[30] K.F. Eckerman, R.W. Leggett, M. Cristy, C.B. Nelson, User's Guide to the DCAL System <https://www.epa.gov/sites/production/files/2015-02/documents/dcal-manual.pdf>, 2006 (accessed 7.4.2017).
[31] D. Smith, M. Stabin, Exposure Rate Constants and Lead Shielding Values for Over 1,100 Radionuclides, Health Phys. 102(3) (2012) 271.
[32] J.S. Bedford, Sublethal damage, potentially lethal damage, and chromosomal aberrations in mammalian cells exposed to ionizing radiations, International Journal of Radiation Oncology, Biology, Physics 21(6) (1991) 1457-1469.
[33] A.A. Edwards, Risks from ionising radiation: deterministic effects, 1998, pp. 175-183.
[34] J. Epstein, D. Harris, Properties of selected radioisotopes. A bibliography, part 1 - Unclassified literature - NASA-SP-7031, Sponsoring Organization: NASA Goddard Space Flight Center, 1968.
[35] L. Urso, J.C. Kaiser, K.G. Andersson, H. Andorfer, G. Angermair, C. Gusel, R. Tandler, Modeling of the fate of radionuclides in urban sewer systems after contamination due to nuclear or radiological incidents, J. Environ. Radioact. 118 (2013) 121-7.
[36] R.C. O'Brien, Radioisotope and Nuclear Technologies for Space Exploration, University of Leicester, 2010.
[37] The Engineering Toolbox, Food and Foodstuff - Specific Heat. <http://www.engineeringtoolbox.com/specific-heat-capacity-food-d_295.html>, (accessed 18.4.2017).
[38] R. Shweikani, M. Hasan, Determination of the optimal measurement counting time and detection limit for gamma-ray spectrometry analysis, Journal for Quality, Comparability and Reliability in Chemical Measurement 20(6) (2015) 501-504.
[39] L.A. Currie, Limits for qualitative detection and quantitative determination: Application to radiochemistry, Anal. Chem. 40(3) (1968) 586-593.
[40] S. Tsroya, B. Dolgin, U. German, O. Pelled, Z.B. Alfassi, Fast determination of 90Sr/90Y activity in milk by Cherenkov counting, Appl. Radiat. Isot. 82 (2013) 332-339.
[41] J. Lehto, X. Hou, Chemistry and analysis of radionuclides : laboratory techniques and methodology, Wiley, Weinheim, 2011.
[42] Food and Drug Administration, Supporting Document for Guidance Levels for Radionuclides in Domestic and Imported Foods. <https://www.fda.gov/food/foodborneillnesscontaminants/chemicalcontaminants/ucm078341.htm>, 2004 (accessed 20.4.2017).
[43] Codex Alimentarius Commission, Codex General Standard for Contaminants and Toxins in Food and Feed (CODEX STAN 193-1995). <http://www.fao.org/fileadmin/user_upload/livestockgov/documents/1_CXS_193e.pdf>, 1995 (accessed 20.4.2017).
[44] A.N. Jones, Density of Milk. <http://hypertextbook.com/facts/2002/AliciaNoelleJones.shtml>, 2002 (accessed 8.4.2017).

[45] R. Belanger, D. Buckley, J. Swenson, Environmental assessment of ionization chamber smoke detectors containing Am-241, Science Applications, Inc., La Jolla, CA (USA), 1979.
[46] The US Food and Drug Adnimistration, Powdered Infant Formula: An Overview of Manufacturing Processes. <https://www.fda.gov/ohrms/dockets/ac/03/briefing/3939b1_tab4b.htm>, (accessed 3.4.2017).
[47] F. Teagasc Food Research Centre, Mark, Infant Formula Processing. <http://daviscofoods.com/as2015/presentations/AS2015_Fenelon.pdf>, (accessed 3.4.2017).
[48] SUEZ, Total Solids Content = Dry Mtter (DM). <https://www.suezwaterhandbook.com/water-and-generalities/water-analysis-and-treatability/sludge-examination/total-solids-content-dry-matter-DM>, (accessed 15.5.2017).
[49] Nestlé, NAN OPTIPRO HA 1 Gold. <http://www.nestle.com.au/brands/baby-toddler-nutrition/nan-infant/nan-optipro-ha-1-gold>, (accessed 15.4.2017).
[50] 明治粉ミルクからセシウム検出　40 万缶無償交換へ, Nikkei Newspaper, Japan, 6.12.2011.
[51] 東京電力福島第一原子力発電所までの直線距離・方位・方位角計算 PAGE. <http://cassiopeia.a.la9.jp/grs/fukushimagenshi.htm>, (accessed 5.5.2017).
[52] 公益財団法人日本分析センター, 平成 25 年度 放射性物質測定調査委託費(浮遊粒子物質測定用テープろ紙の放射性物質による大気中放射性物質濃度把握)事業報告書. <http://radioactivity.nsr.go.jp/ja/contents/10000/9771/24/tape_1.pdf>, 2014 (accessed 3.4.2017).
[53] D. Velić, M. Bilić, S. Tomas, M. Planinić, Energy saving in spray drying process, Integrated Systems for Agri-food Production-In the process of European Integration-, 2003.
[54] Japan Meteorological Agency, 月ごとの値. <http://www.data.jma.go.jp/obd/stats/etrn/view/monthly_a1.php?prec_no=43&block_no=1070&year=2011&month=3&day=&view=>, (accessed 10.5.2017).
[55] ANVAL VALVES PVT LTD, Bulk Density Chart. <http://www.anval.net/downloads/bulk%20density%20chart.pdf>, (accessed 5.4.2017).
[56] J.H. Hubbell, S.M. Seltzer, X-Ray Mass Attenuation Coefficients, National Institute of Atandards and Technology, 1996.
[57] R.D. Lloyd, C.W. Mays, D.R. Atherton, G.N. Taylor, 90Sr + 90Y bremsstrahlung efficiency predicted for humans, Radiation and environmental biophysics 13(3) (1976) 229.
[58] A. Ho, S. Witharana, G. Jonkmans, L. Li, R. Surette, J. Dubeau, X. Dai, Detection of bremsstrahlung radiation of Sr-90-Y-90 for emergency lung counting, Radiat. Prot. Dosim. 151(3) (2012) 443-449.
[59] A.P. Packer, D. Larivière, C. Li, M. Chen, A. Fawcett, K. Nielsen, K. Mattson, A. Chatt, C. Scriver, L.S. Erhardt, Validation of an inductively coupled plasma mass spectrometry (ICP-MS) method for the determination of cerium, strontium, and titanium in ceramic materials used in radiological dispersal devices (RDDs), Anal. Chim. Acta 588(2) (2007) 166-172.
[60] D.Ø. Eriksen, Senior advisor at the University of Oslo. Personal communication, (2017).
[61] R.A. Penneman, T.K. Keenan, The radiochemistry of americium and curium, National Academies1960.
[62] R. Přibil, Analytical Applications of EDTA and Related Compounds: International Series of Monographs in Analytical Chemistry, Elsevier2013.
[63] P. Kofstad, i. Universitetet i Oslo Kjemisk, K 102 Uorganisk kjemi : kompendium : Del 1 : Hovedgruppenes elementer, Kjemisk institutt. Universitetet i Oslo, Oslo, 1977.
[64] L.H. Hihara, R.P. Adler, R.M. Latanision, Environmental degradation of advanced and traditional engineering materials, CRC Press2013.
[65] J. Emery, G. Leddicotte, The radiochemistry of gold, National Academies1961.
[66] J.P. Omtvedt, Professor in Chemistry at the University of Oslo. Personal communication, 2017.
[67] S. Agostinelli, et al., Geant4—a simulation toolkit, Nuclear Inst. and Methods in Physics Research, A 506(3) (2003) 250-303.
[68] J. Allison, et al., Recent developments in Geant4, Nuclear Inst. and Methods in Physics Research, A 835 (2016) 186-225.

[69] J. Allison, et al., Geant4 developments and applications, Nuclear Science, IEEE Transactions on 53(1) (2006) 270-278.
[70] Extech Instruments Corporation (A FLIR Company), FLIR i60. <https://www.instrumart.com/assets/i60-datasheet.pdf>, 2010 (accessed 15.5.2017).
[71] S. Everts, A Brief History of Chemical War. <https://www.chemheritage.org/distillations/magazine/a-brief-history-of-chemical-war>, 2015 (accessed 5.11.2017.).
[72] F. Frischknecht, The history of biological warfare, EMBO reports 4(S1) (2003) S47-S52.
[73] V. Fenopetov, B. Lawlor, T. Japaridze, Y. Tsantoulis, A. Schmid, New Security Threats—Old Security Architecture and Mind-Sets: Countering the Threat of Radiological and Nuclear Terrorism in the Black Sea Region, American Foreign Policy Interests 33(5) (2011) 197-208.
[74] YaleGlobal Online, C.E.B. Choksy, J.K. Choksy, WMD Proliferation Threatens the World. <http://yaleglobal.yale.edu/content/wmd-proliferation-threatens-world>, 4.5.2013 (accessed 7.5.2017).
[75] The Center for Food Security & Public Health, Plague. <cfsph.iastate.edu/Factsheets/pdfs/plague.pdf >, (accessed 10.5.2017).
[76] The Center for Food Security & Public Health, Anthrax. <http://www.cfsph.iastate.edu/Factsheets/pdfs/anthrax.pdf>, (accessed 10.5.2017).
[77] S.L. Hoenig, SpringerLink, Compendium of Chemical Warfare Agents, Springer New York2007.
[78] T.K. Ghosh, M.A. Prelas, D.S. Viswanath, S.K. Loyalka, Science and technology of terrorism and counterterrorism, CRC Press2009.
[79] M.J. Berger, J.S. Coursey, M.A. Zucker, J. Chang, ESTAR: Stopping Power and Range Tables for Electrons, National Institute of Standards and Technology, 1998.

Appendix

Appendix A: Definitions

The following definitions and concepts are used throughout this work:

Syndrome – Medical term for when illness is present.

Symptom – Medical term for an indication of a symptom.

Threshold for syndrome – Dose when a given rate of persons exposed to this condition will contract a given syndrome (illness). In this work, the condition is limited to only when a certain amount of radiation has been absorbed, both internally and externally.

Mortality – Conditions that lead to early death.

Morbidity – Conditions that are non-lethal.

Hematopoietic syndrome – Syndrome caused due to blood cells that are killed by radiation. The syndrome is also known as bone marrow syndrome. Symptoms of the syndrome include bleeding and inability to fight infection [33].

Gastrointestinal syndrome – Syndrome caused due to gut cells that are killed by radiation. Symptoms of the syndrome include vomiting, diarrhea and gastrointestinal bleeding [33].

Prodromal syndromes –Syndrome caused due to absorbing radiation in the head and trunk (torso) areas. The term used to describe specific symptoms that may indicate the onset of disease. The symptoms include anorexia, nausea, fatigue, vomiting and diarrhea [33].

Absorbed dose – Energy of radiation deposited to a given organ. Unit of Gy is used.

Absorbed dose rate coefficient for ingestion – Coefficient used to convert a given activity of radionuclide in Bq ingested to absorbed dose of a given organ. Unit of Gy/day·Bq is used. The coefficient is given for each day since the day of ingestion.

Absorbed dose rate coefficient for external exposure - Coefficient used to convert a given activity of radionuclide in Bq placed as a point source to absorbed dose rate of a whole body. Unit of Gy/h·Bq is used.

Total absorbed dose – Sum of absorbed dose received since the first ingestion of a radionuclide until the day specified.

Daily absorbed dose – Absorbed dose received on the day specified due to ingestion of a radionuclide on day 1.

Single serving – Amount of IMF fed to an infant per time. 24.6 g is assumed.

Daily serving – Amount of IMF fed to an infant per day. 103.5 g is assumed.

Consecutive serving – Multiple amount of IMF fed to an infant. Single serving or daily serving of specified times.

Selected level – Activity concentration in IMF given from the activity at the time of contamination specified in **Table 26**.

Mortality level – Activity concentration in IMF of which the absorbed dose received from ingesting one serving reaches the threshold of hematopoietic syndrome in 7 days after the ingestion.

Morbidity level - Activity concentration in IMF of which the absorbed dose received from ingesting one serving reaches the threshold of prodromal syndrome in 7 days after the ingestion.

MDA level - Activity concentration in IMF of which the activity level is the minimum detectable in a laboratory setting.

Permissible level - Activity concentration in IMF of which the activity level is equal to the DIL and GL given from FDA and CAC, respectively.

Appendix B: List of Abbreviations

CAC – Codex Alimentarius Commission

DIL – Derived Intervention Level

FDA – US Food and Drug Administration

GL – Guideline Level

IMF –Infant Milk Formula

MDA –Minimum Detectable Activity

RBE – Relative Biological Effectiveness

RDD – Radiological Dispersion Devices

RTG –Radioisotope Thermoelectric Generator

Appendix C: List of Coefficients

Table 21: Radiation yield used in this work is shown for each material and for the energy of β particles in MeV when reaching the material [79].

Material	Energy of β particle (keV)	Radiation yield
Iron	400	8.489×10^{-3}
Water	800	2.928×10^{-3}

Table 22: Mass stopping power in MeV·cm^2/g, used in this work, is shown for each material for the energy of β particles in MeV when reaching in the material. Density of each material in g/cm^3 is also shown [79].

Material	Energy of β particle (keV)	Mass stopping power (MeV·cm^2/g)	Density of material
Air	350	1.984	1.225×10^{-3}
Lithium	800	1.551	0.534
Tin	500	1.256	7.31
Water	800	1.896	1

Table 23: Mass absorption coefficient in cm^2/g, used in this work, is shown for the energy of γ rays in keV when reaching the material. Density of each material in g/cm^3 is also shown [56].

	Energy of photons (keV)	Mass absorption coefficient (cm^2/g)	Density (g/cm^3)
Air (dry)	60	1.875×10^{-1}	1.225×10^{-3}
	600	8.055×10^{-2}	
Iron	50	1.958	7.874
	60	1.205	
	600	7.704×10^{-2}	
Lithium	60	1.438×10^{-1}	0.534
	600	6.968×10^{-2}	
Tin	60	6.564	7.31
	600	8.113×10^{-2}	
Water (liquid)	50	0.2269	1.00
	60	0.2059	
	600	8.956×10^{-2}	

Table 24: Absorbed dose rate coefficients for ingestion used in this work in Gy/day/Bq are shown for each radionuclide and for each syndrome. The coefficients are given for each day from day 1 to day 7. Day 1 is the day the specified radionuclide is ingested. The coefficients are originally given for different organs in the reference [29].

Nuclide	Syndrome	Absorbed dose rate coefficient (Gy/day/Bq) on the specified day since ingestion of radionuclide on day 1						
		1	2	3	4	5	6	7
^{90}Sr	Gastrointestinal	4.55×10^{-5}	5.31×10^{-5}	3.37×10^{-5}	1.83×10^{-5}	9.18×10^{-6}	5.71×10^{-6}	3.57×10^{-6}
	Hematopoietic	1.89×10^{-6}	3.31×10^{-6}	4.10×10^{-6}	4.63×10^{-6}	5.01×10^{-6}	5.19×10^{-6}	5.35×10^{-6}
	Prodromal	5.22×10^{-5}	5.34×10^{-5}	3.41×10^{-5}	1.86×10^{-5}	9.59×10^{-6}	6.14×10^{-6}	4.00×10^{-6}
^{137}Cs	Gastrointestinal	2.83×10^{-6}	3.12×10^{-6}	3.14×10^{-6}	3.09×10^{-6}	2.98×10^{-6}	2.89×10^{-6}	2.77×10^{-6}
	Hematopoietic	7.53×10^{-7}	7.56×10^{-7}	7.25×10^{-7}	6.95×10^{-7}	6.64×10^{-7}	6.41×10^{-7}	6.12×10^{-7}
	Prodromal	8.75×10^{-6}	4.75×10^{-6}	4.71×10^{-6}	4.59×10^{-6}	4.41×10^{-6}	4.27×10^{-6}	4.09×10^{-6}
^{241}Am	Gastrointestinal	3.04×10^{-5}	2.78×10^{-5}	1.35×10^{-5}	5.85×10^{-6}	2.24×10^{-6}	1.05×10^{-6}	3.96×10^{-7}
	Hematopoietic	9.21×10^{-7}	1.40×10^{-6}	1.49×10^{-6}	1.53×10^{-6}	1.54×10^{-6}	1.54×10^{-6}	1.54×10^{-6}
	Prodromal	3.56×10^{-5}	2.79×10^{-5}	1.36×10^{-5}	5.89×10^{-6}	2.27×10^{-6}	1.07×10^{-6}	4.10×10^{-7}

Table 25: Two different absorbed dose rate coefficients for external exposure used in this work, exposure rate constant in $C\cdot m^2/kg\cdot Bq\cdot h$ and f-factor in $Gy\cdot kg/C$ are shown for each radionuclide. The coefficients are originally given in $C\cdot m^2/kg\cdot Bq\cdot s$ and cGy/R, respectively, in the reference [31].

Radionuclide	Exposure rate constant ($C\cdot m^2/kg\cdot Bq\cdot h$)	Conversion factor ($Gy\cdot kg/C$)
^{137}Cs	2.39×10^{-15}	37.29
^{156m}Tb	2.07×10^{-16}	33.95
^{241}Am	5.22×10^{-16}	36.12